Tracking

Giacomo BRUNO

Center for Cosmology Particle Physics and Phenomenology (CP3)

Université catholique de Louvain (UCL), Louvain-la-Neuve, Belgium

Giacomo.Bruno@uclouvain.be

Goals of tracking

- Crossing points of charged particles from tracking detectors

- Identify charged particles (e,μ,π,k,p,ions, Σ,Ξ,Ω, τ,D,B,)
  - From compatibility of **position measurements** with a particle trajectory ("track")
- Measure their momentum
  - From trajectory and its bending in a magnetic field

- Input to higher-level reconstruction (use of several tracks, several detectors or detector information other than position)
  - Vertices (points of multiple track generation)
  - Muons and electrons: id and measurements
  - b-jet identification ("b-tagging")
  - Jet measurement with particle-flow algorithms
  - Particle identification with Cherenkov light, dE/dx, TOF, transition radiation
  - Detector calibration and alignment

- Physics data analysis

- Lecture 1:
Tracking detectors

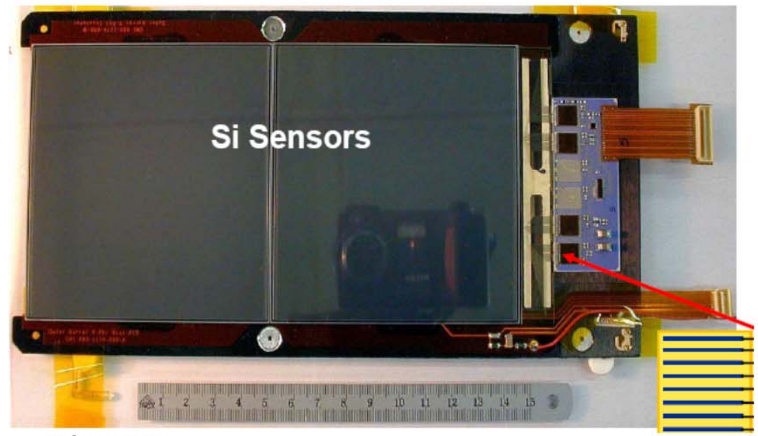

- Lecture 2:
Tracking algorithms

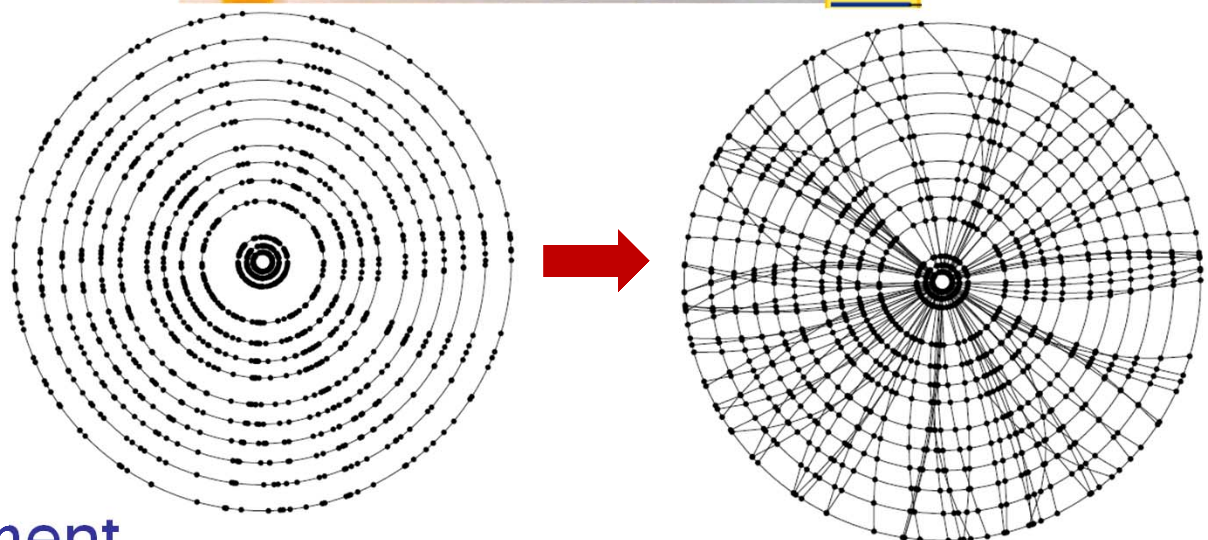

- Lecture 3:
Vertexing and alignment

TRACKING DETECTORS

- Interactions
- Gas detectors
- Solid state detectors

Interactions

Ionization

- Elastic collisions with the electrons of the medium
  - So frequent that energy loss can be described as a continuous process (Bethe-Bloch formula)
  - If $M >> m_e$, direction is almost unaffected.

[see e.g. PDG 2010]

Ionization:

$$-\left\langle \frac{dE}{dx} \right\rangle = K z^2 \frac{Z}{A} \frac{1}{\beta^2} \left[\frac{1}{2} \ln \frac{2 m_e c^2 \beta^2 \gamma^2 T_{max}}{I^2} - \beta^2 - \frac{\delta(\beta\gamma)}{2} \right] \quad [\cdot \rho]$$

density

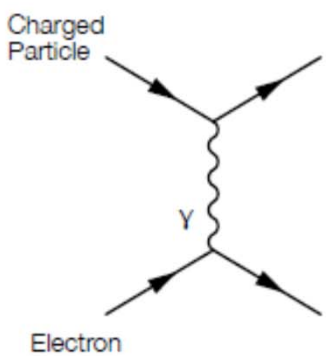

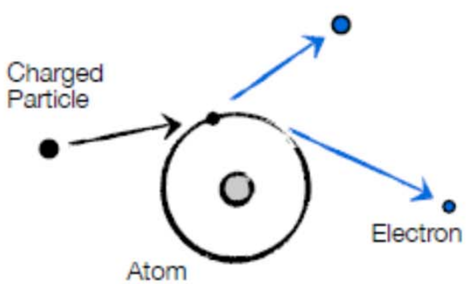

$K = 4\pi N_A r_e^2 m_e c^2 = 0.307$ MeV g^{-1} cm^2

$T_{max} = 2 m_e c^2 \beta^2 \gamma^2 / (1 + 2\gamma m_e/M + (m_e/M)^2)$

[Max. energy transfer in single collision]

z	:	Charge of incident particle
M	:	Mass of incident particle
Z	:	Charge number of medium
A	:	Atomic mass of medium
I	:	Mean excitation energy of medium
δ	:	Density correction [transv. extension of electric field]

$N_A = 6.022 \cdot 10^{23}$
[Avogardo's number]

$r_e = e^2/4\pi\varepsilon_0 m_e c^2 = 2.8$ fm
[Classical electron radius]

$m_e = 511$ keV
[Electron mass]

$\beta = v/c$
[Velocity]

$\gamma = (1-\beta^2)^{-2}$
[Lorentz factor]

Validity:

$.05 < \beta\gamma < 500$

$M > m_\mu$

Ionization

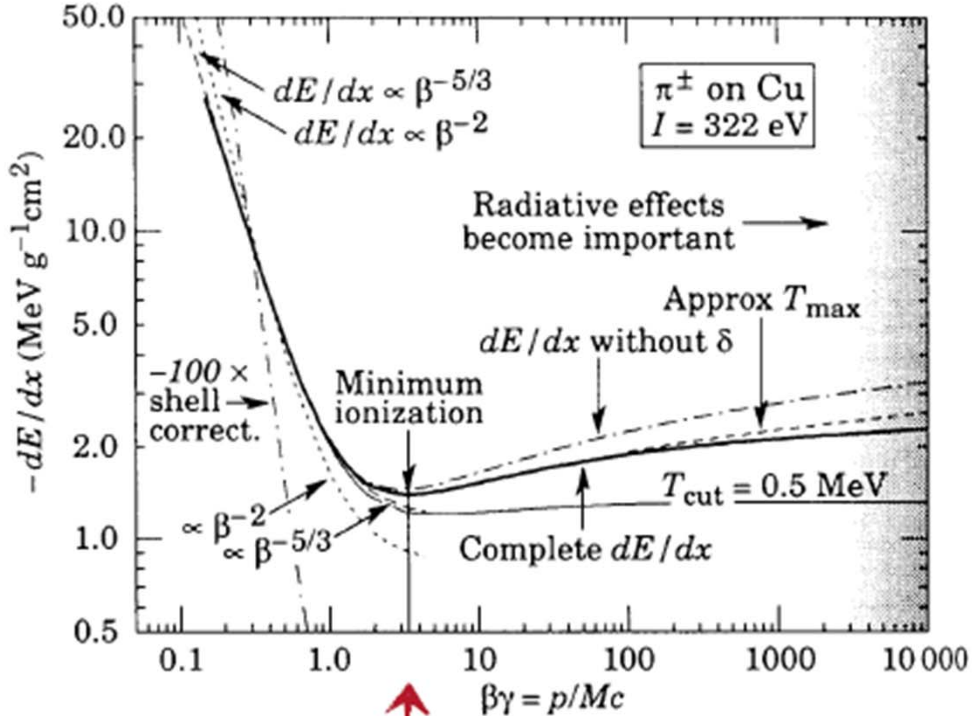

$\beta\gamma$ = 3-4

Minimum ionizing particles (MIP): $\beta\gamma$ = 3-4

dE/dx falls ~ β^{-2}; kinematic factor
[precise dependence: ~ $\beta^{-5/3}$]

dE/dx rises ~ $\ln(\beta\gamma)^2$; relativistic rise
[rel. extension of transversal E-field]

Saturation at large ($\beta\gamma$) due to density effect (correction δ)
[polarization of medium]

Units: MeV g^{-1} cm^2

MIP looses ~ 13 MeV/cm
[density of copper: 8.94 g/cm^3]

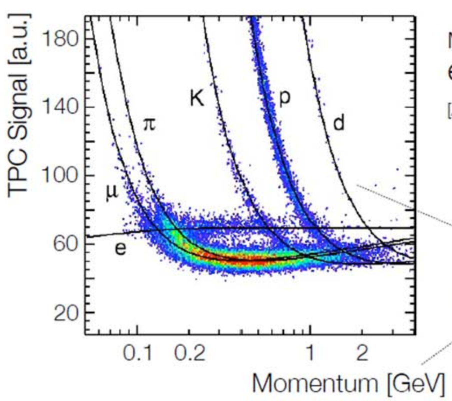

Measured energy loss
[ALICE TPC, 2009]

Bethe-Bloch

Remember:
dE/dx depends on β!

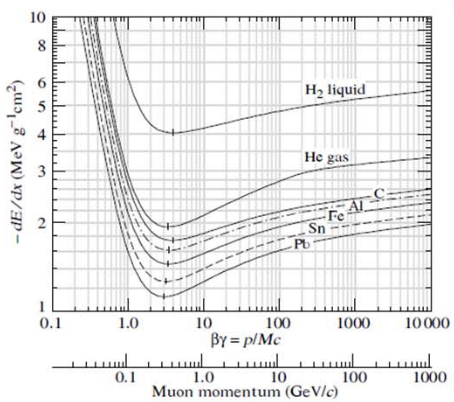

ng

Minimum ionization:

ca. 1 - 2 MeV/g cm^{-2}
[H$_2$: 4 MeV/g cm^{-2}]

Energy loss fluctuations

- Bethe-Bloch gives the mean of the energy loss
  - Fluctuations described by Landau-Vavilov distribution
- For thin layers (< few mm) Most Probable Value is strongly shifted toward lower values
  - Long tail due to rare energetic δ-rays (up to several GeV)
  - → the mean is ill-defined to describe **deposits** in thin absorbers
  - Relativistic rise is also dumped

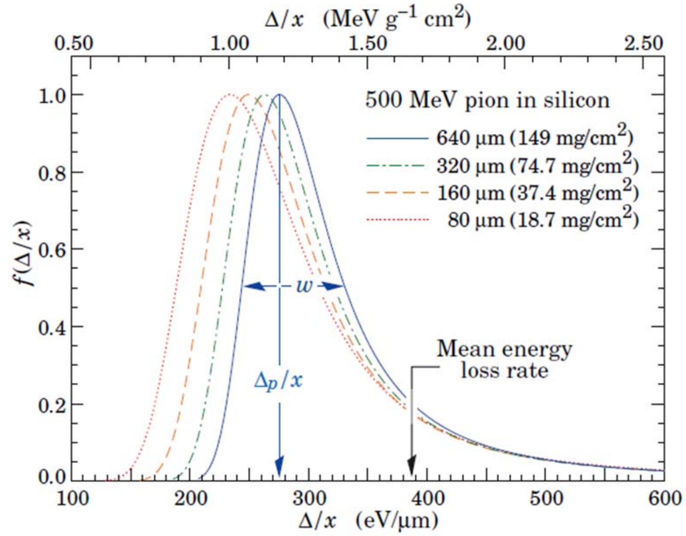

Figure 30.8: Straggling functions in silicon for 500 MeV pions, normalized to unity at the most probable value δ_p/x. The width w is the full width at half maximum.

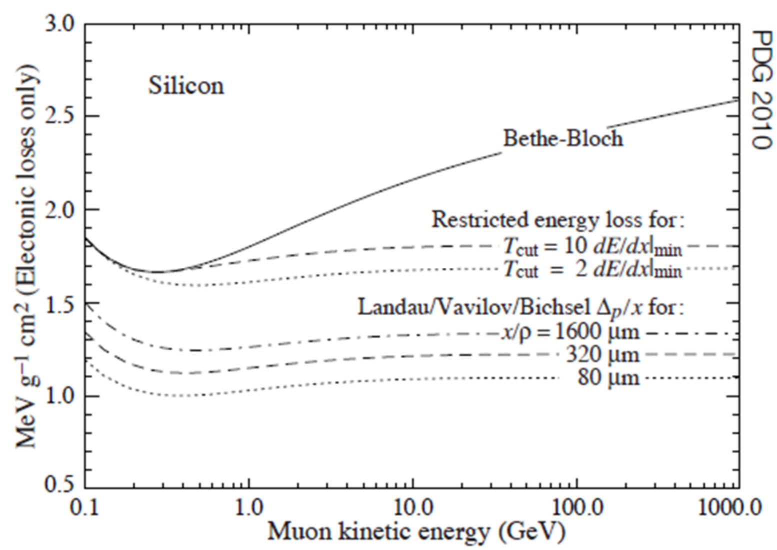

Bethe-Bloch dE/dx, two examples of restricted energy loss, and the Landau most probable energy per unit thickness in silicon. The change of Δ_p/x with thickness x illustrates its a ln x + b dependence. Minimum ionization ($dE/dx|_{min}$) is 1.664 MeV g^{-1} cm^2. Radiative losses are excluded. The incident particles are muons.

Electrons: bremsstrahlung

- Very little change in Bethe-Bloch
- Energy loss at HEP energies is dominated by bremsstrahlung
  - Rare, catastrophic process

$$-\left\langle \frac{dE}{dx} \right\rangle_{\mathrm{el.}} = K \frac{Z}{A}\frac{1}{\beta^2}\left[\ln \frac{m_e \beta^2 c^2 \gamma^2 T}{2I^2} + F(\gamma)\right]$$

[T: kinetic energy of electron]

$$-\left\langle \frac{dE}{dx} \right\rangle = K z^2 \frac{Z}{A}\frac{1}{\beta^2}\left[\frac{1}{2}\ln \frac{2m_e c^2 \beta^2 \gamma^2 T_{\max}}{I^2} - \beta^2 - \frac{\delta(\beta\gamma)}{2}\right]$$

Critical energy:

$$\left.\frac{dE}{dx}(E_c)\right|_{\mathrm{Brems}} = \left.\frac{dE}{dx}(E_c)\right|_{\mathrm{Ion}} \qquad E_c^{\mathrm{Gas}} = \frac{710\ \mathrm{MeV}}{Z+0.92} \qquad E_c^{\mathrm{Sol/Liq}} = \frac{610\ \mathrm{MeV}}{Z+1.24}$$

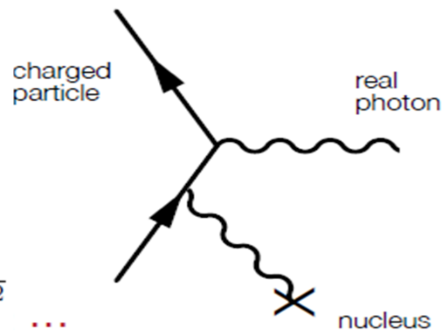

Bremsstrahlung arises if particles are accelerated in Coulomb field of nucleus

$$\frac{dE}{dx} = 4\alpha N_A \frac{z^2 Z^2}{A}\left(\frac{1}{4\pi\epsilon_0}\frac{e^2}{mc^2}\right)^2 E \ln\frac{183}{Z^{\frac{1}{3}}} \propto \frac{E}{m^2} \ \ldots$$

i.e. energy loss proportional to $1/m^2$ → main relevance for electrons ...

... or ultra-relativistic muons

Consider electrons:

$$\frac{dE}{dx} = 4\alpha N_A \frac{Z^2}{A} r_e^2 \cdot E \ln\frac{183}{Z^{\frac{1}{3}}}$$

$$\frac{dE}{dx} = \frac{E}{X_0} \quad \text{with} \quad X_0 = \frac{A}{4\alpha N_A Z^2 r_e^2 \ln\frac{183}{Z^{\frac{1}{3}}}}$$

[Radiation length in g/cm²]

$$\rightarrow E = E_0 e^{-x/X_0}$$

After passage of one X_0 electron has lost all but $(1/e)^{th}$ of its energy

[i.e. 63%]

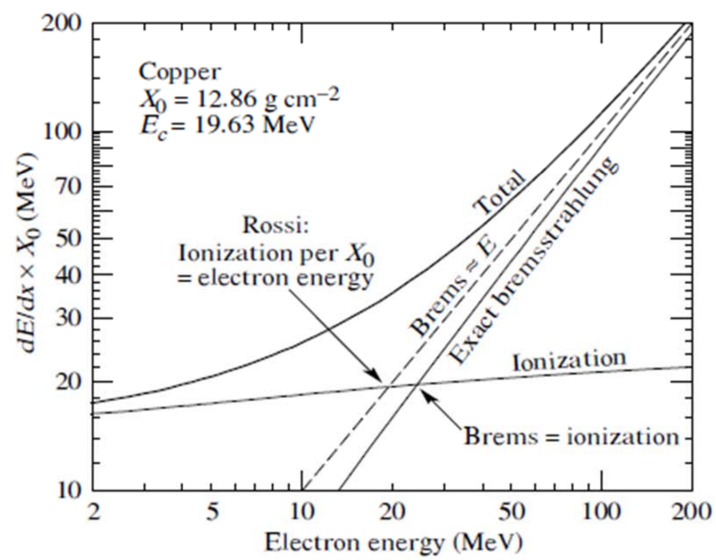

High-energy muons

- Radiative losses by bremmstrahlung, e^-e^+ pair production and nuclear interactions
- Contrary to electrons must go through massive parts of the detector in order to improve momentum measurement
  - Problem for tracking (will see later)

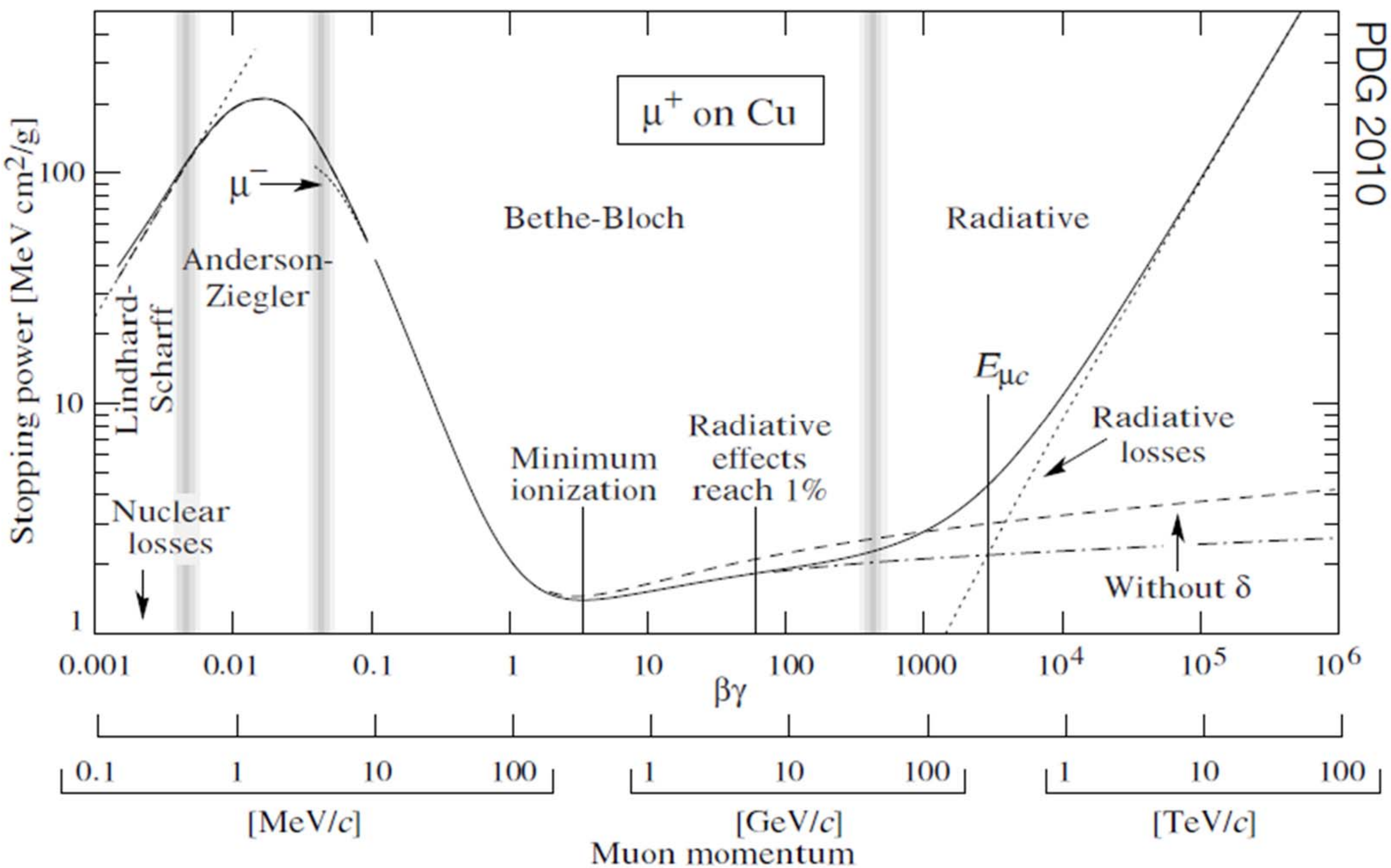

Multiple scattering

- Elastic collisions with nuclei of the medium – analogy with collisions in classical physics leads to the conclusion
  - Negligible contribution to energy loss
  - Dominant contribution to change in direction
    - Fundamental factor for tracking
  - Can be described as a continuous process

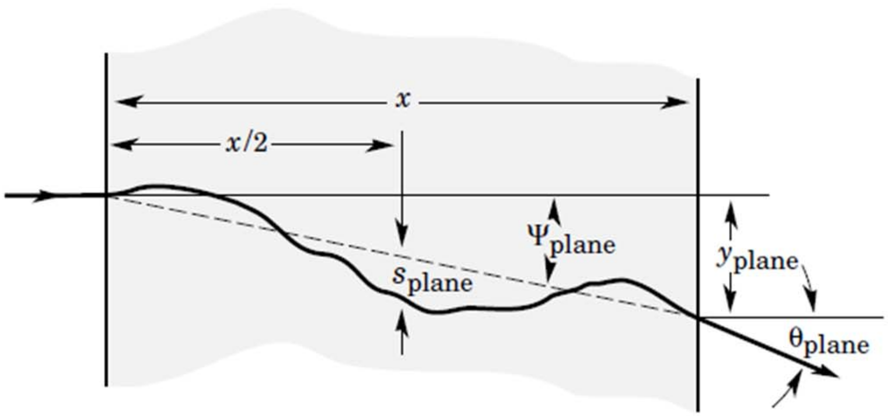

Figure 30.10: Quantities used to describe multiple Coulomb scattering. The particle is incident in the plane of the figure.

$$\theta_0 = \theta_{\text{plane}}^{\text{rms}} = \frac{1}{\sqrt{2}}\theta_{\text{space}}^{\text{rms}} \qquad \theta_0 = \frac{13.6\ \text{MeV}}{\beta c p}\, z\, \sqrt{x/X_0}\Big[1 + 0.038\ln(x/X_0)\Big]$$

GAS DETECTORS

Single-wire proportional chamber

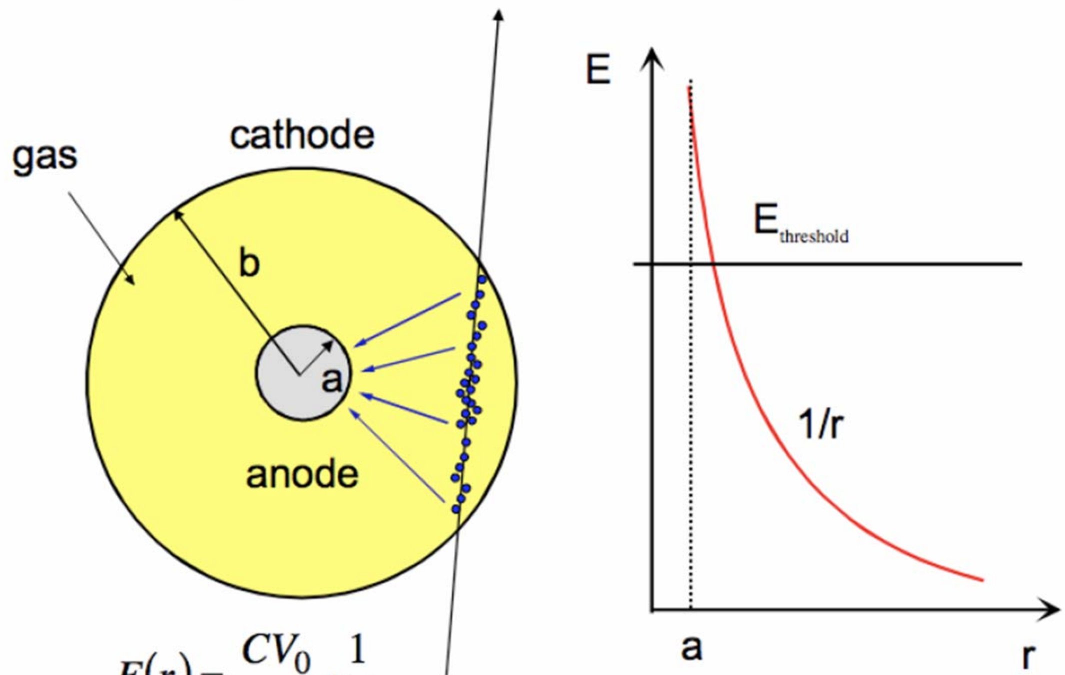

$$E(r) = \frac{CV_0}{2\pi\varepsilon_0} \cdot \frac{1}{r}$$

$$V(r) = \frac{CV_0}{2\pi\varepsilon_0} \cdot \ln\frac{r}{a} \qquad C = \text{capacitance / unit length}$$

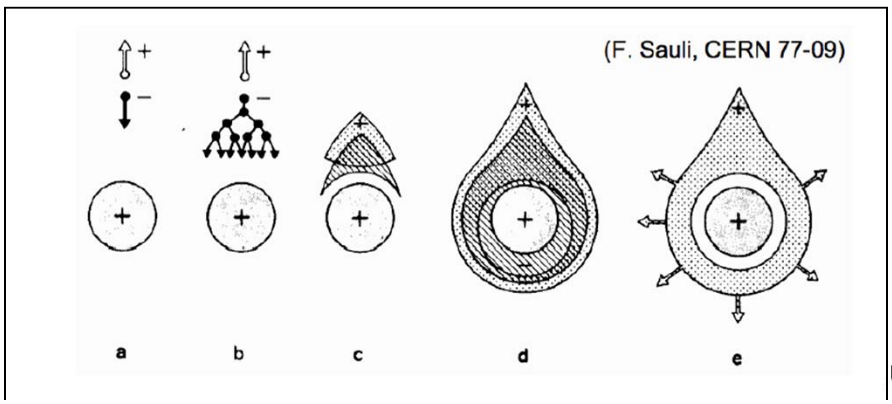

- Particle passage through gas creates electrons – ions pairs
- Electrons drift toward anode wire
  - Drift distance ~ O (1 cm)
  - Wire diameter ~ O(10-100 μm)
- As they approach the wire the electric field increases and accelerates electrons
- Charge multiplication (avalanche) starts for E~O(10 kV/cm)
  - New e-ion pairs produced
  - $N=n_0\exp(\alpha(E)x)$
- Electric signal induced on electrodes
  - Due to displacement of charge
  - Ions gives useful signal (electrons too fast and too little distance covered)

Gas gain

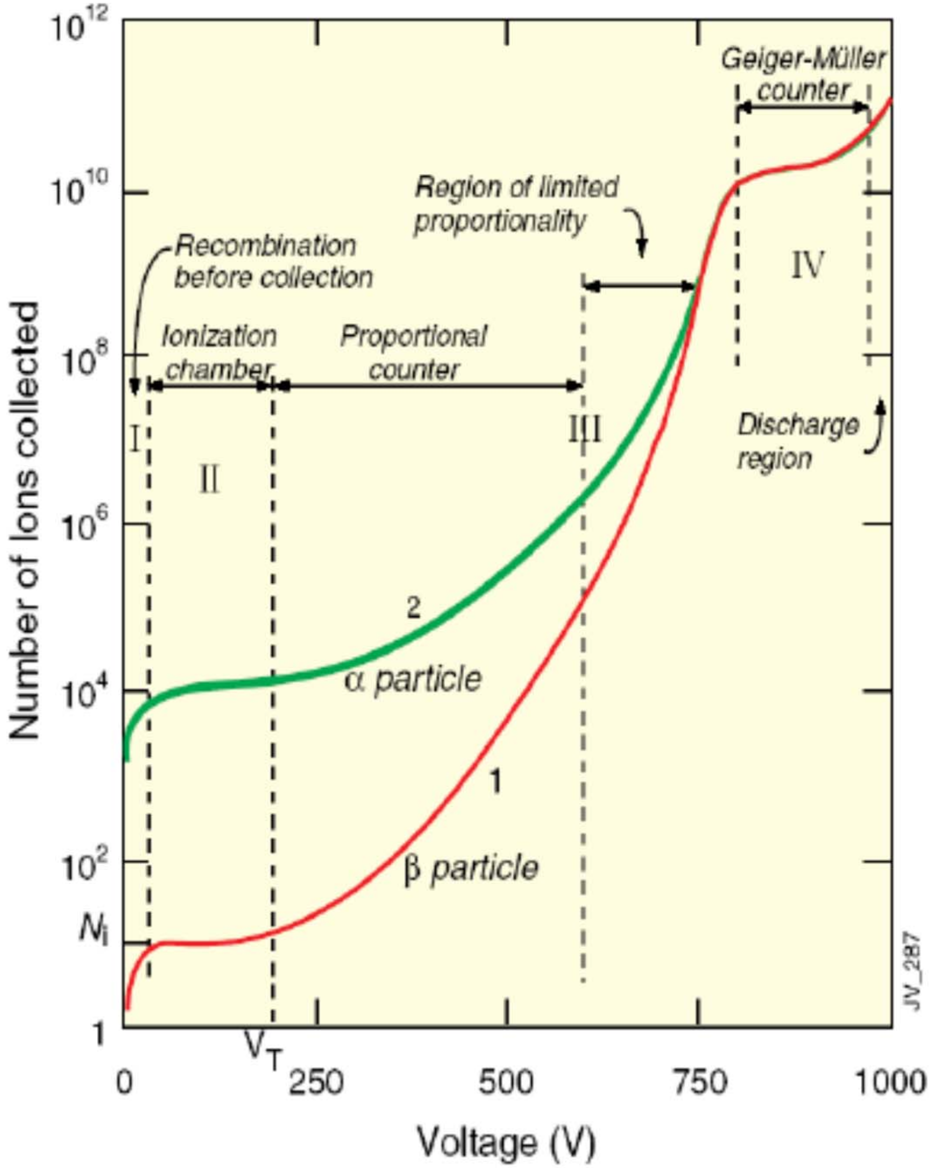

Depending on intensity of electric field:

- Ionization mode
  - No primary charge amplification
- Proportional mode
  - Signal proportional to primary charge
- Streamer mode
  - Strong photoemission from e – ion recombination
  - Still, no need to switch off HV to stop discharge
- Geiger mode
  - Massive photemission, this additional ionizations and avalanches
  - Full length of wire interested by avalanches
  - Need to cut off HV

Evolution: multiwire proportional chamber

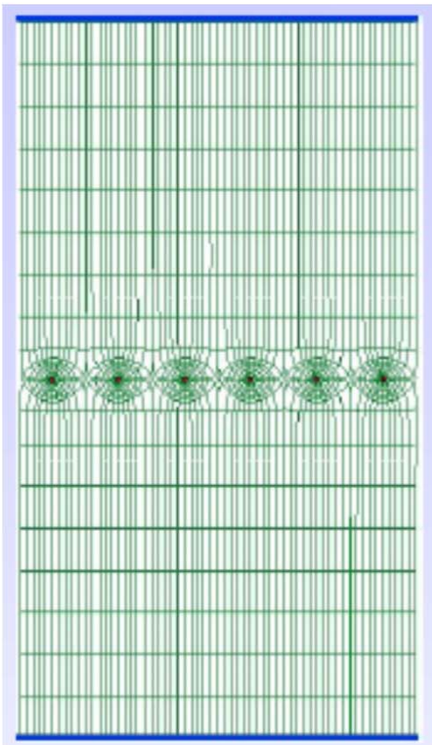

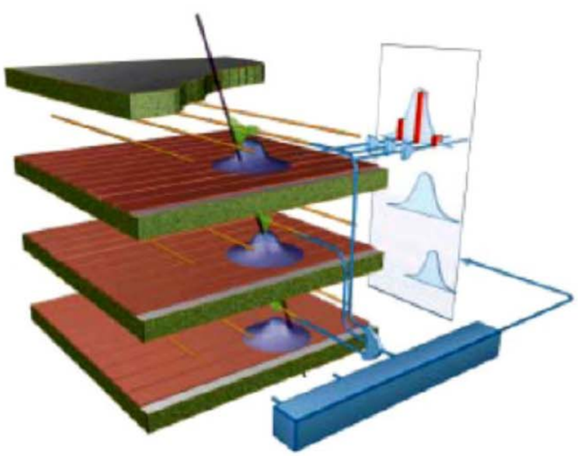

- Multiple wires in a single gas volume
  - Interwire distance (pitch) ~ O(1 -10 mm)
- Space resolution
  - Digital readout: pitch/√12
  - Analog readout: much better
    - But need additional electrodes (Strips or pads)
- Nobel prize to G. Charpak

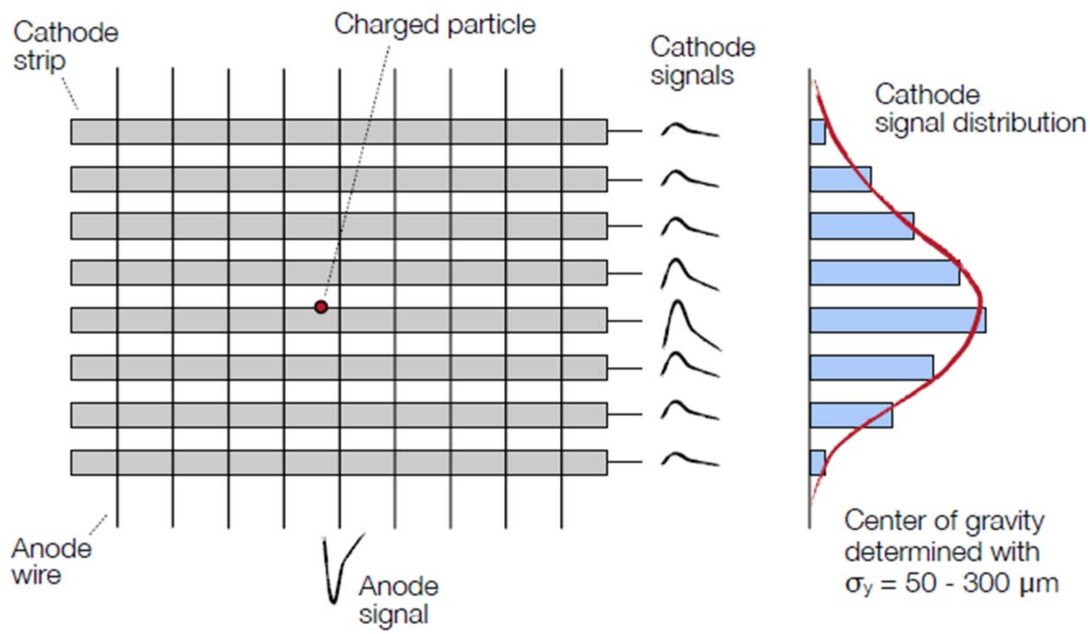

Drift chamber

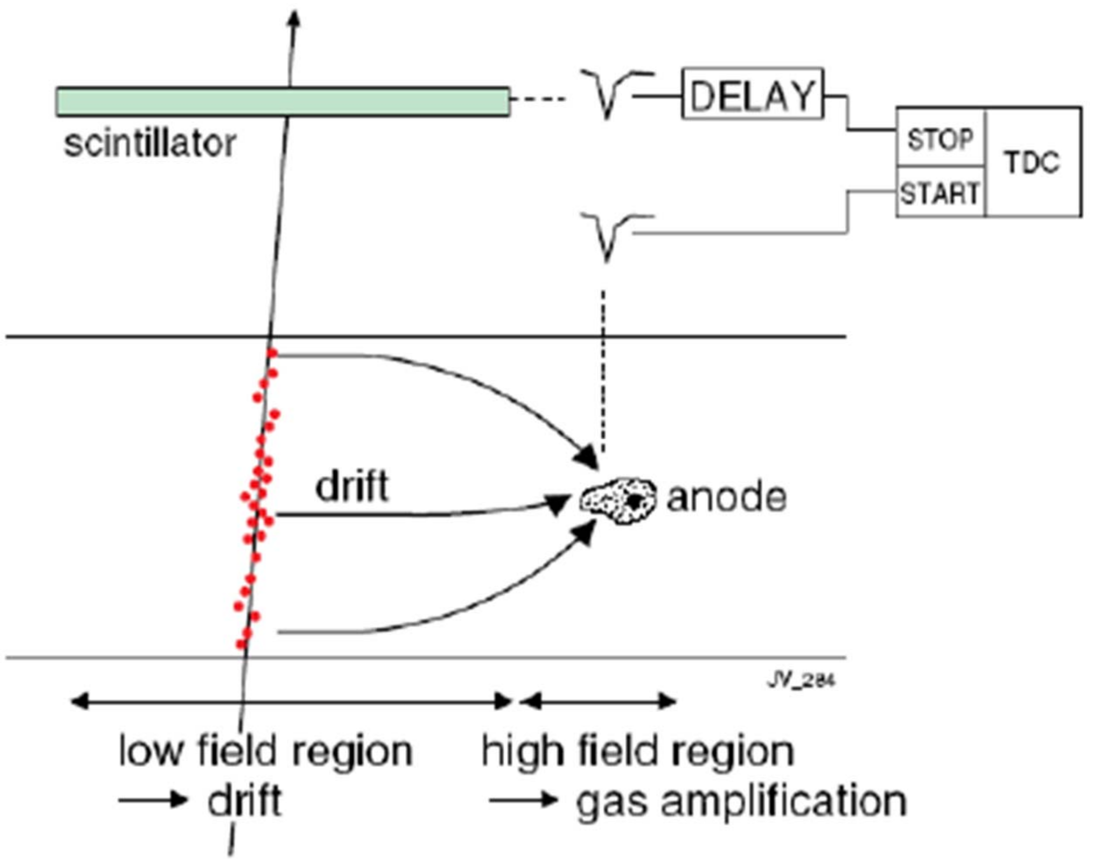

- Position information by measuring electron drift time
    - Drift velocity: O(10-100 μm/ns)
- Need external signal providing particle arrival time
- Large coverage with small number of electronic channels
- Suffers in busy environments and in the presence of magnetic fields

Drift chambers at the LHC

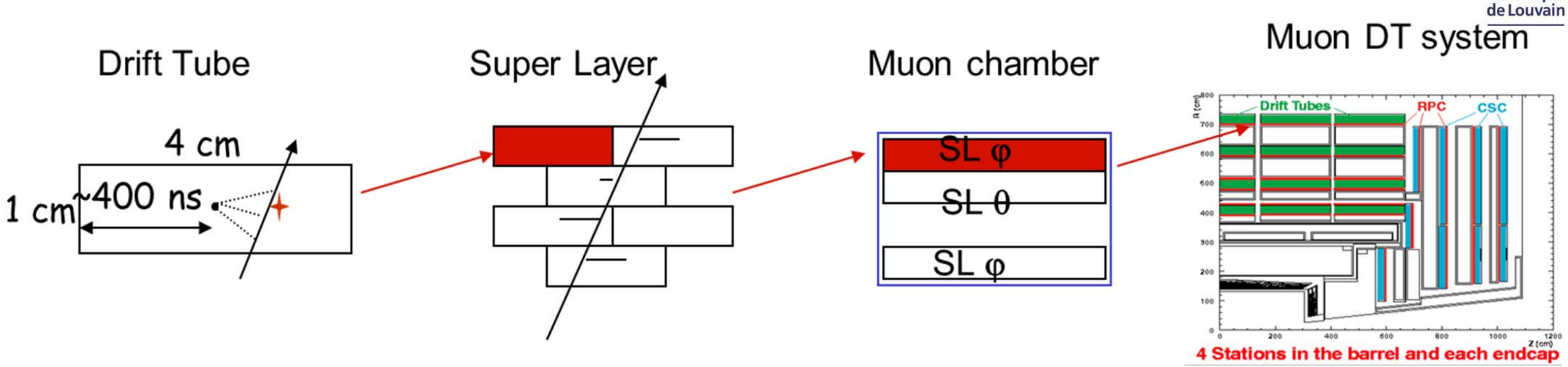

- T0= absolute time of the bunch crossing at which TDC starts counting. It counts from 0 to 1000 ns and then starts again. Start happens in coincidence with one bunch crossing.
- N=number of bunch crossings, after T0, at which the muon is produced at the vertex
- T0 + N x BXT + T_flight + T_drift_i + T_sigdelay = T0 + T_meas_i (x 4)
- 5 unknowns: 4 T_drift_i and N ; 4 measurements T_meas_i:
- X_i = V_drift x T_drift_i
- Y = A X + B ; 1 equation in 2 unknowns to be satisfied by 4 points
- 8 equations/constraints in 7 unknowns. Find out best estimates of the unknown from fit to measurements. Chi^2 minimization.
- Can also work if there are only 3 measurements out of 4. In this case one has 6 equations/constraints in 6 unknowns. It stops working with only 2 measurements.

Time projection chamber (TPC)

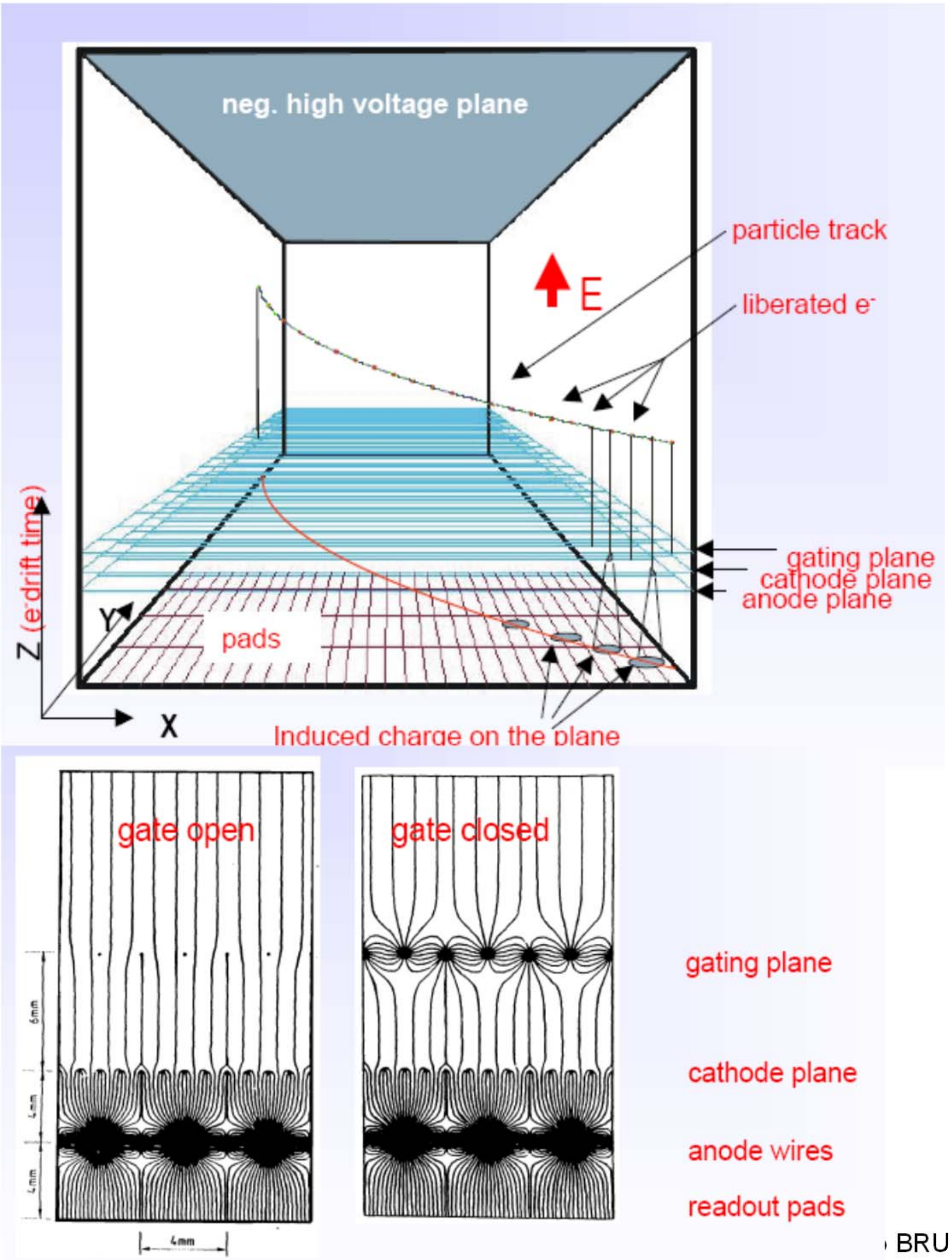

- 3-dim track reco
  - combines principles of drift and multiwire proportional chamber in a single detector
- Gating plane
  - Avoids gas multiplication when no external trigger signal
  - Avoids ion diffusion in the main drift region (field distortions)

ALICE TPC

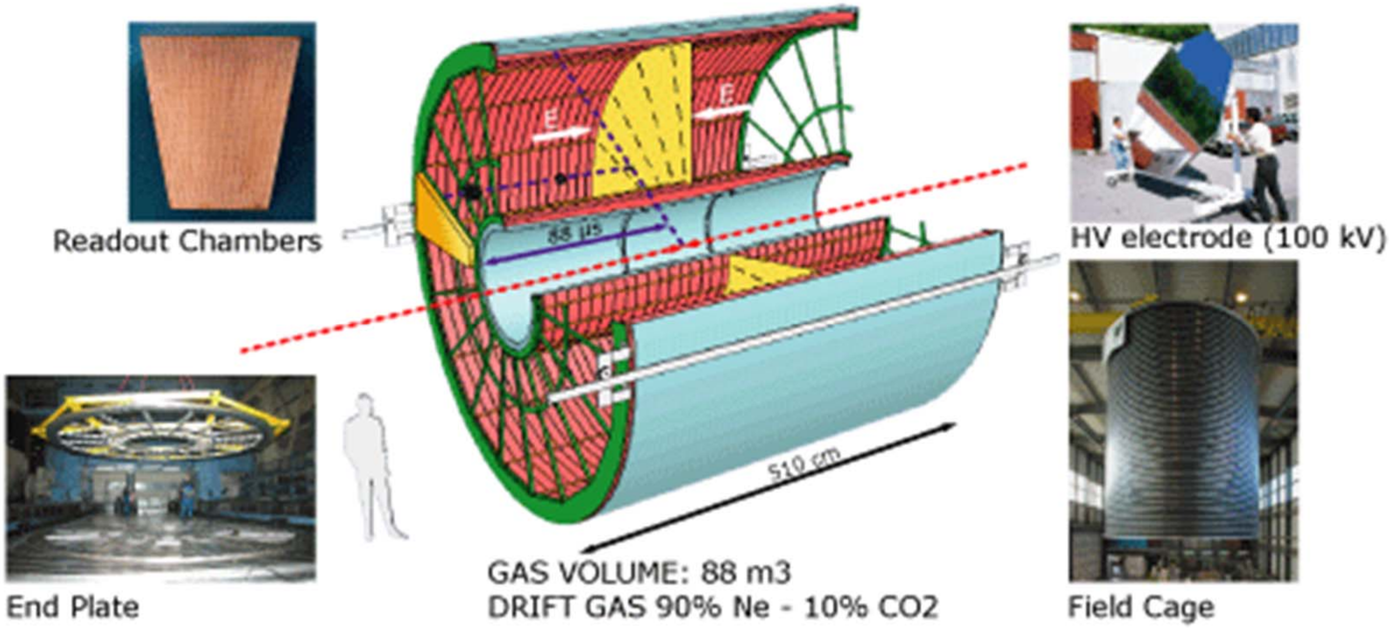

- ~5 m diameter. ~5 m height
- O(500 k) pads on cylinder base
  - 7 x 4.5 mm^2 each
- 2.5 m max drift length (~100 us drift time)
- E^{drift}~400 V/cm
- Anode wire spacing: ~2.5 mm
- Anode wire diameter: 20 um

Micro-Strip Gas Chamber (MSGC)

- Replaces wires with microstructures on dielectric materials
  - ❑ Simpler construction
    - Wires must be very thin, strung at high tension, ageing problem
  - ❑ Improved stability and flexibility (strips, pads, …)
  - ❑ Improved rate capability
    - Ions drift over very small distances (~ 100 um)

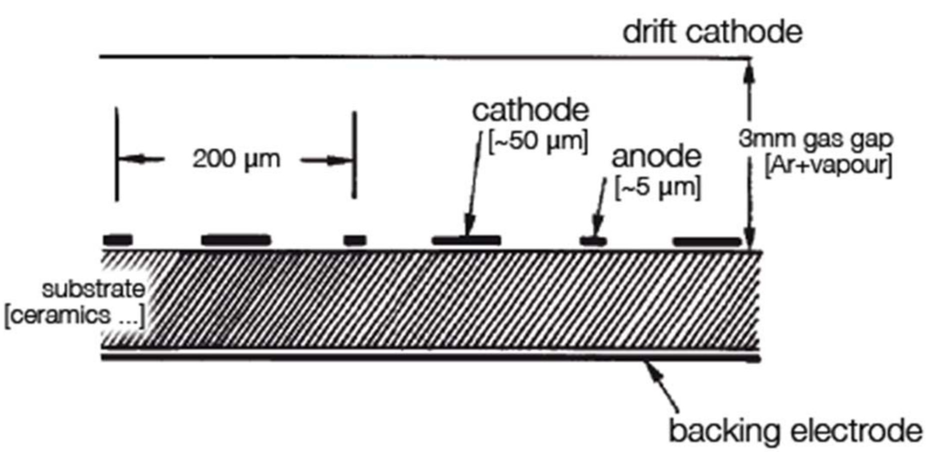

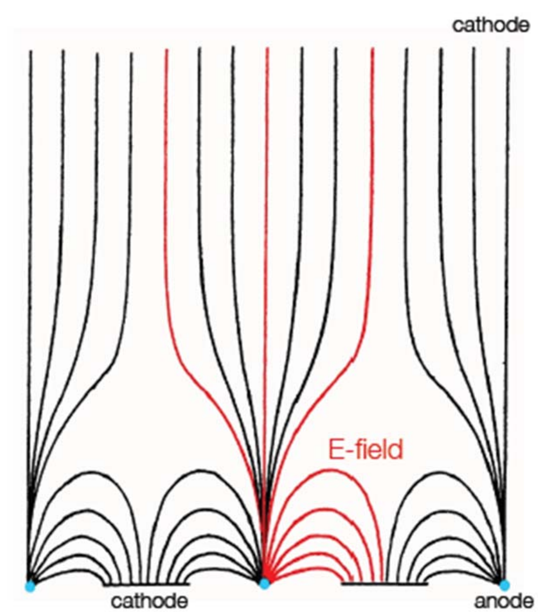

Micromegas and GEM

- Reduce further path for ions with intermediate grids
  - Further improve rate capability

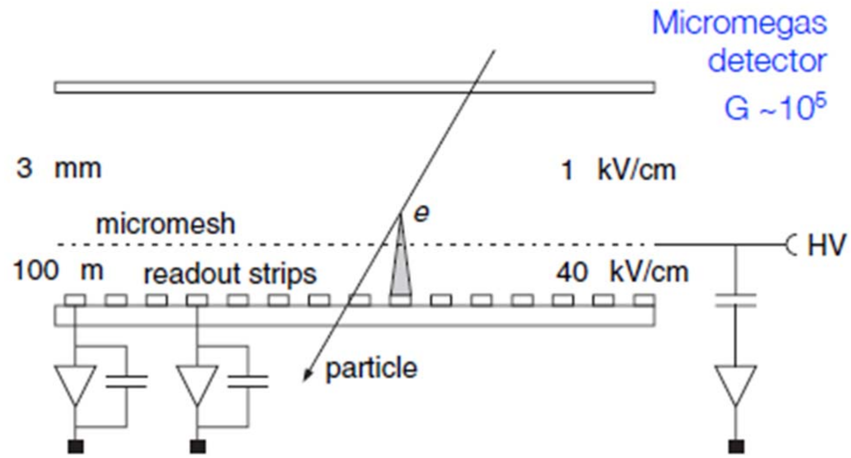

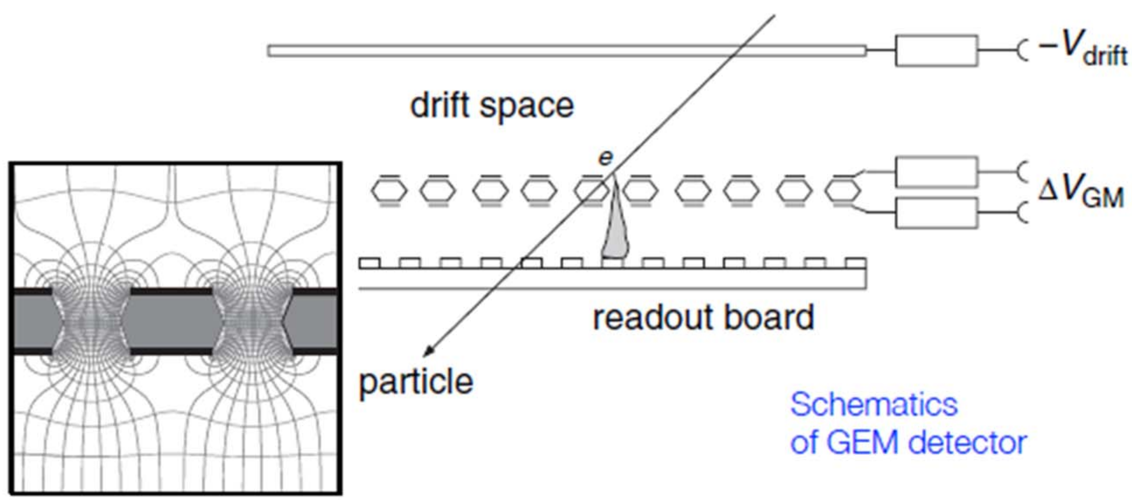

Planar-electrode detectors

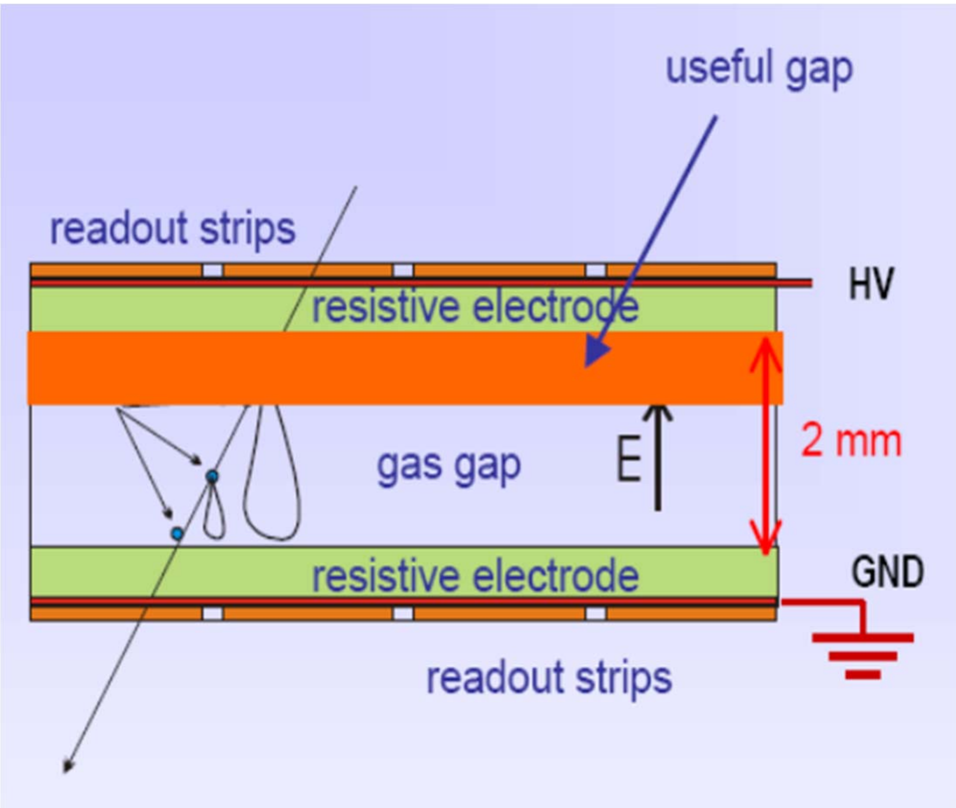

- Ex: Resistive Plate Chamber
  - Planar electrode geometry
  - Avalanche multiplication starts immediately (V~10kV over d~2 mm)
  - Signal induced on strips or pads electrodes
  - Excellent time resolution
  - Simple construction
  - Poor space resolution (>1 mm) compared to wire detectors
    - Space extension of avalanche

Gas detectors: summary

- Gas detectors – general
  - +Small perturbation of primary particles
  - +Low cost per unit surface
  - +Flexible geometry
  - Position resolution: O(>100 um) with wires
  - - ageing (due to large charge involved, discharges, chemical reactions)
  - - rate capability
    - Limited by evacuation of ion charge (field distortions, primary electron capture)
    - Solution: reduce path for ions
      - MicroMEGAS, MSGC, GEM

SOLID STATE DETECTORS

Solid state material structure

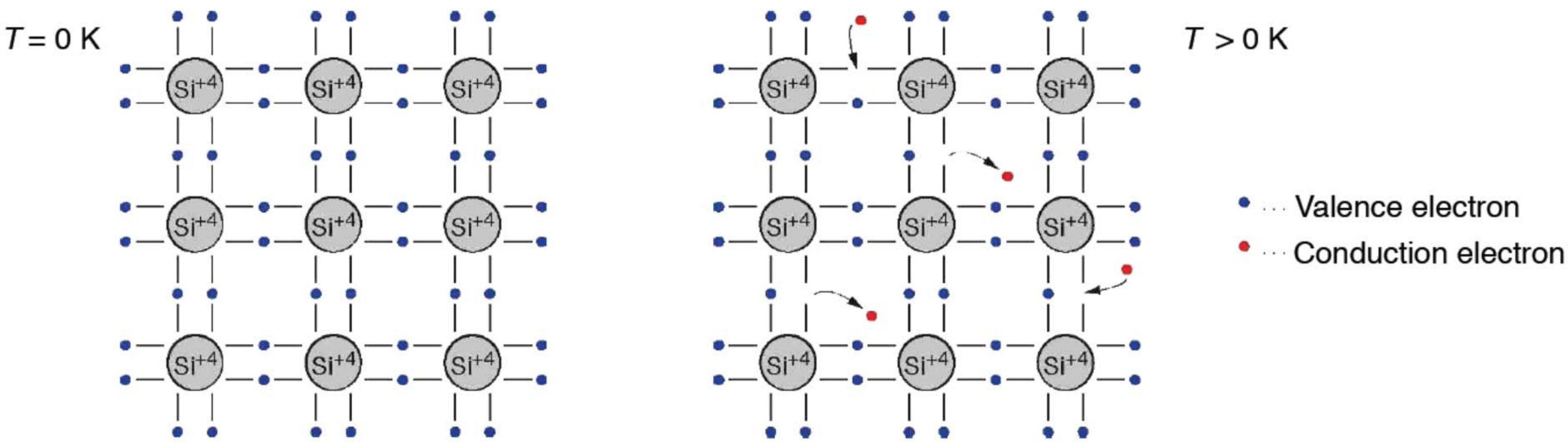

- Each silicon atom has 4 closest neighbors, the 4 electrons in the outer shell are shared and form covalent bonds.
- At low temperature all electrons are bound
- At higher temperature thermal vibrations break some of the bonds and the free electrons provide conductivity: **electron conduction**
- The remaining open bonds can be filled by close-by valence electrons (pushed by an electric field) such that the “holes” change position: **hole conduction.**

Energy levels structure

- In an isolated atom the electrons have only discrete energy levels.
- In solid state material the atomic levels merge to energy bands.
- In metals the conduction and the valence band overlap, whereas in isolators and semiconductors these levels are separated by an energy gap (band gap). In isolators this gap is large.

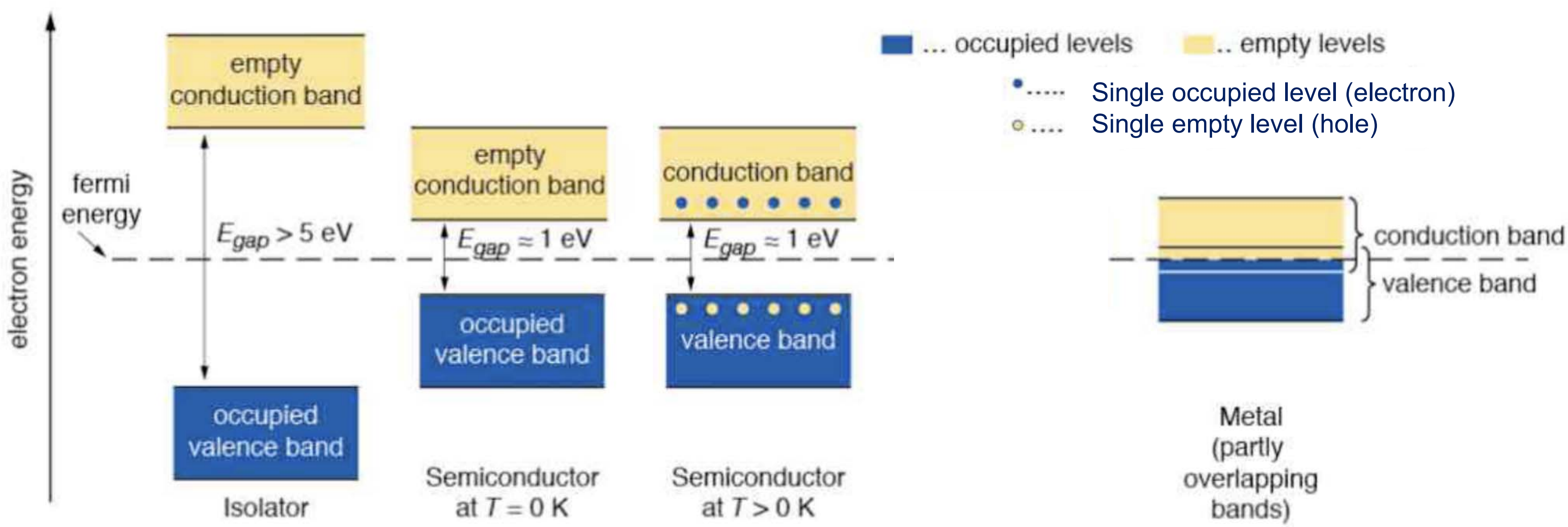

Semiconductor data

	Diamond	SiC (4H)	GaAs	Si	Ge
Atomic number Z	6	14/6	31/33	14	32
Bandgap E_g [eV]	5.5	3.3	1.42	1.12	0.66
E(e-h pair) [eV]	13	7.6-8.4	4.3	3.6	2.9
density [g/cm^3]	3.515	3.22	5.32	2.33	5.32
e-mobility μ_e [cm^2/Vs]	1800	800	8500	1450	3900
h-mobility μ_h [cm^2/Vs]	1200	115	400	450	1900

Detecting particles

- In a pure semiconductor (no impurities), the density of electrons in the conduction band, *n*, is equal to the density of holes in the valence band, *p.*
  - In silicon at room temperature:
    - n=p= 1.45 10^{10} cm^{-3} free charge carrier density
    - # atoms = 10^{22} cm^{-3}

- Increasing the gas gap (going for insulators) reduces thermal noise (reduces n and p), but reduces the signal from a MIP too (more energy required to create an electron-hole pair. Optimal gap is given by diamond, but still …
- Must find a different way to reduce the number of free charge carriers

n-doping

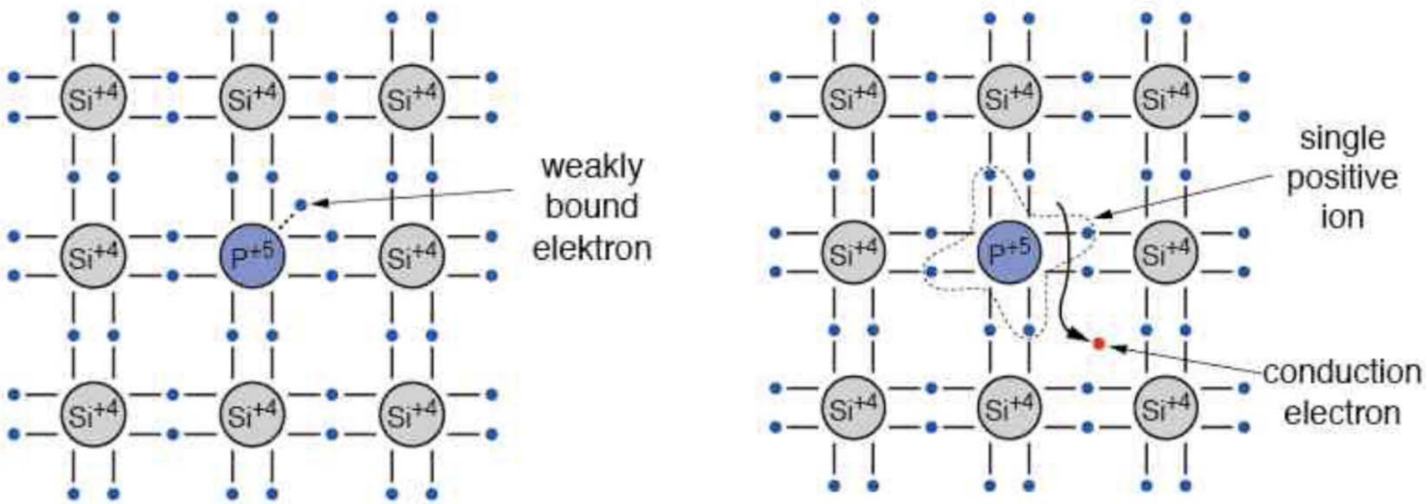

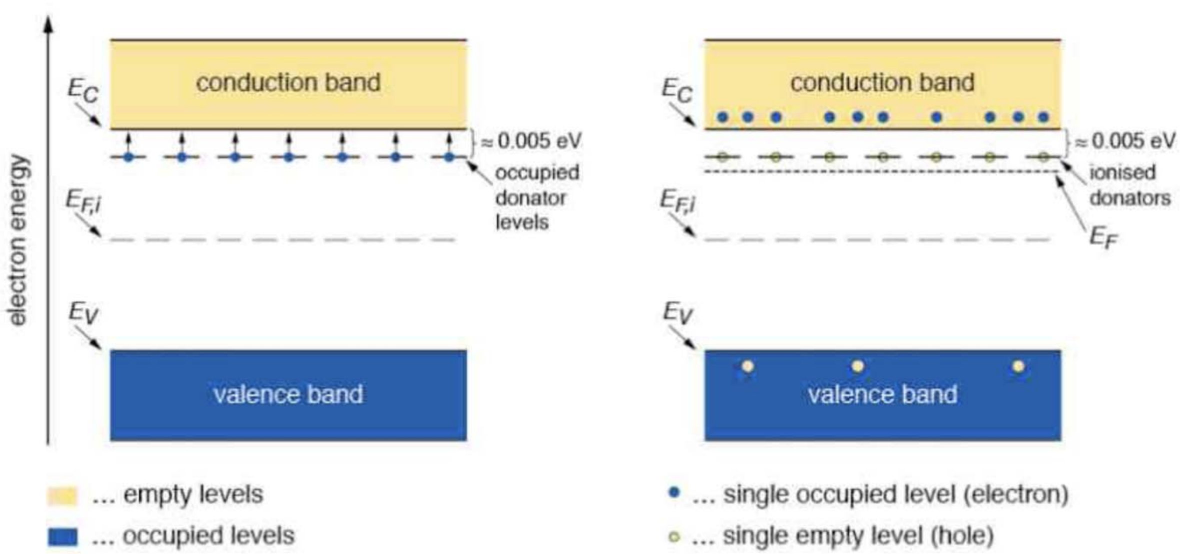

- Add "donor" atoms with 5 valence e^-
  - P, As, Ga, Sb
- 5^{th} valence e^- is weakly bound and can easily abandon the atom to become a free charge carrier

p-doping

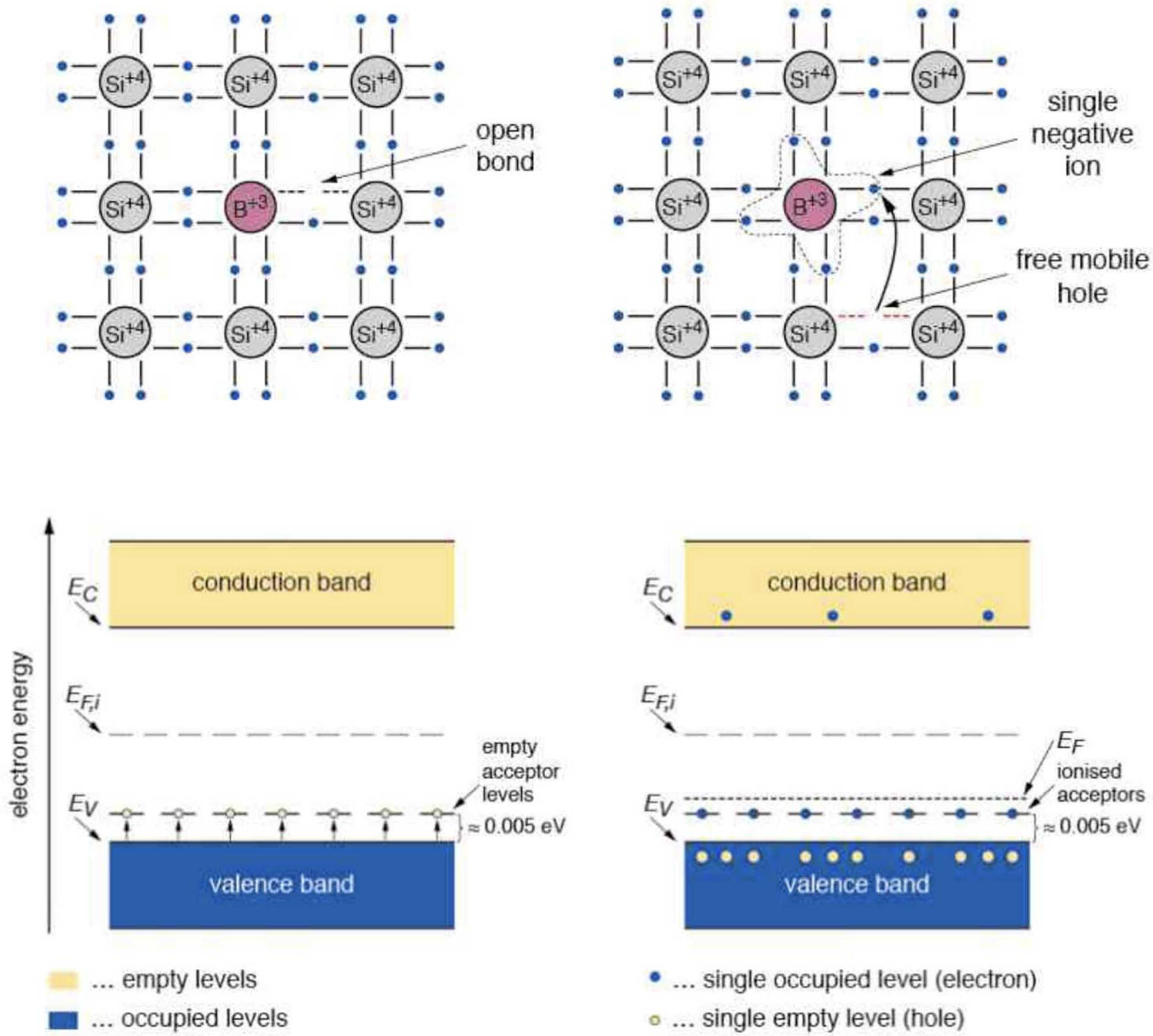

- "acceptor" atoms with 3 valence e$^-$
  - B, Al, Ga, In
- Acceptors attract near-by e$^-$ and produce holes

p-n junction

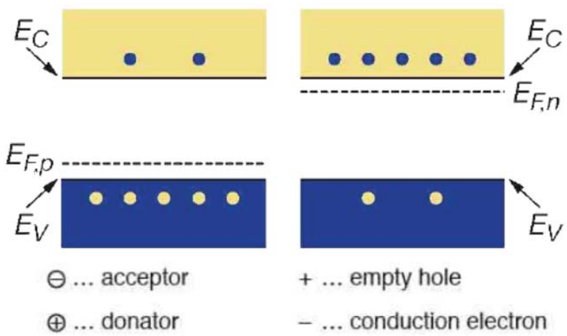

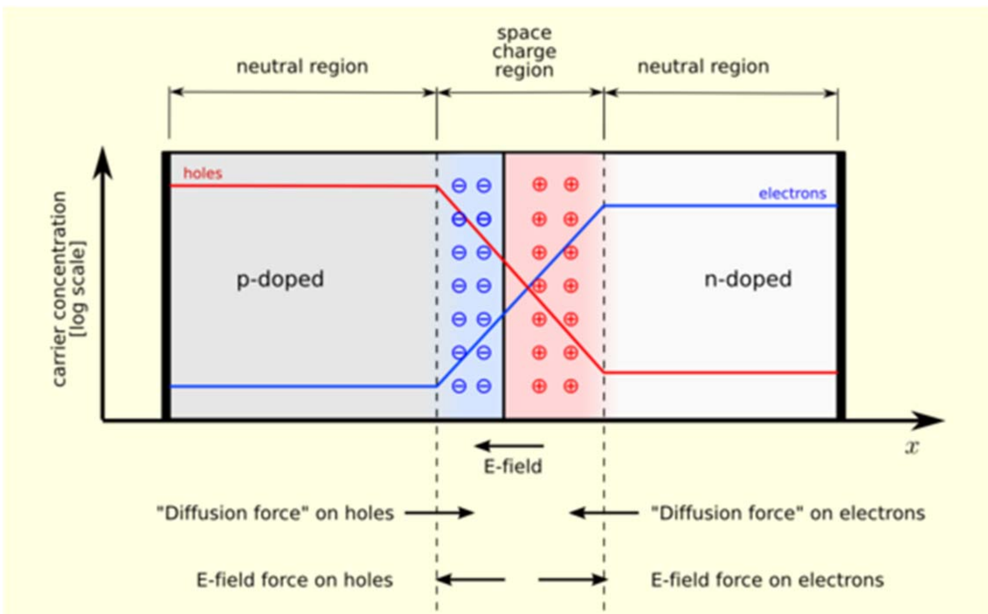

- At the junction between an n-type and p-type semiconductor:
  - Conduction e$^-$ diffuse from n- to p-type zone and recombine with holes there.
  - Holes diffuse from p- to n-type zone and recombine with e$^-$
  - net static charge remains in the region of the junction
    - An E-field is generated that counters diffusion until equilibrium is reached
- Junction region gets depleted of free charge carriers
  - Depletion zone extends more over region less doped

p-n junction with reverse bias

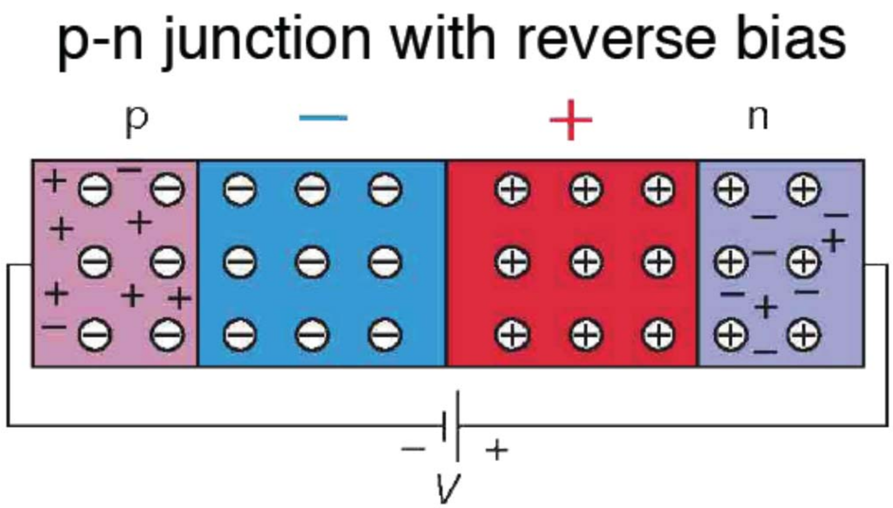

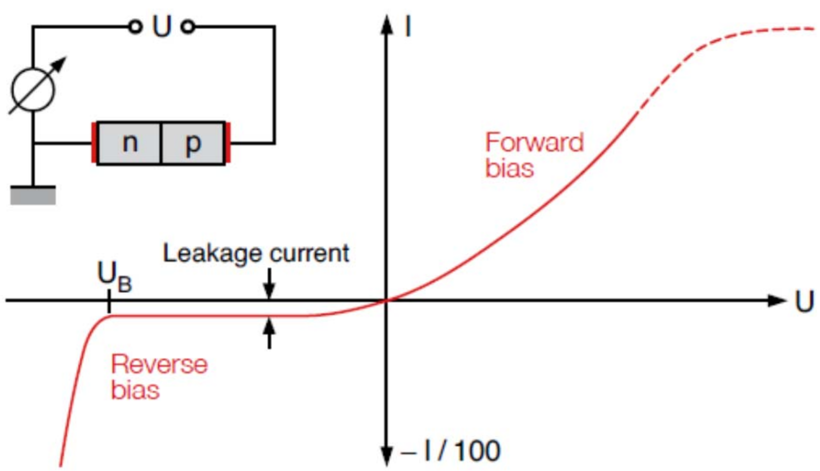

- reverse bias operation: external voltage with anode connected to n-type region
- Potential difference across junction increases
  - Static charge must increase → depletion zone extends further
- This is the operation mode of a semiconductor detector

Semiconductor detector

- Segmentation
  - Strips, pads, pixels
- Typical parameters
  - Thickness: 150-500 um
  - Strip pitch: 20-150 um
  - Strip length: O(10 cm)
  - Pixel size: 100 x 100 um^2
  - Charge collection: 20 ns
  - Operating voltage: O(100 V)
- Output signal
  - dE/dx(MIP)=300 eV/um; Si: 3.6 eV/pair → 80 e-h pairs per um → 25000 pairs/MIP

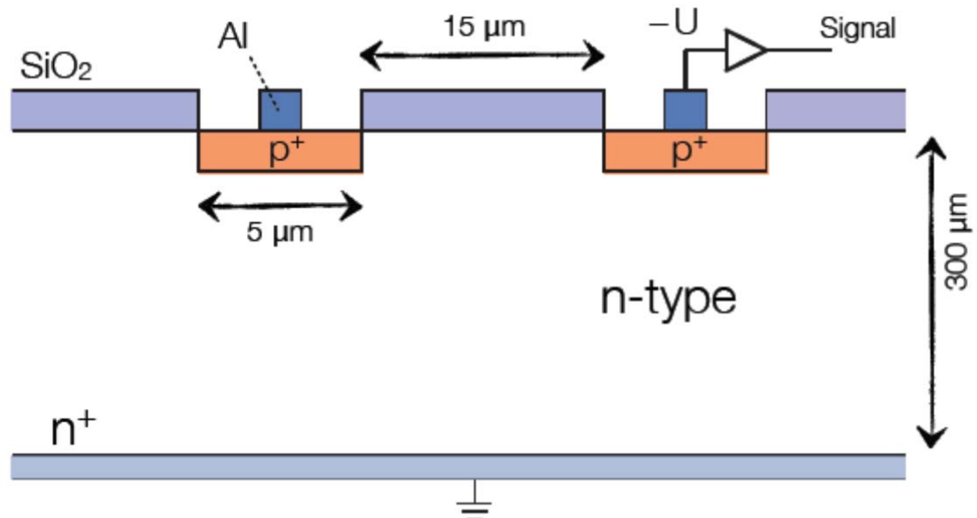

- Structure configuration
  - n-doped substrate
  - Heavily p-doped thin layer on one side
    - Depletion zone extends fully on n side
  - Heavily n-doped thin layer on opposite side
    - Just for ohmic contact

Detector space resolution

- Calculate center of gravity of collected charges
  - Single strip clusters: pitch/√12
- Factors to take into account
  - δ-rays shift center of gravity
  - Landau fluctuations
  - Charge diffusion
  - Lorentz drift in magnetic fields
  - Noise
    - Leakage current
    - Det capacitance (better with small strips/pixels)
    - Front-end electronics and bias voltage components

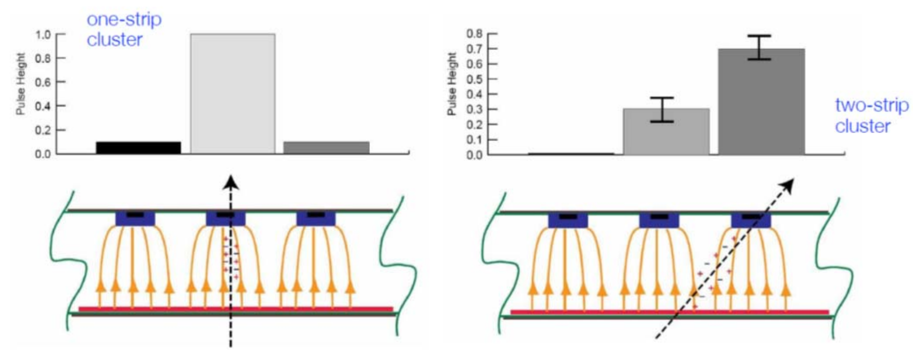

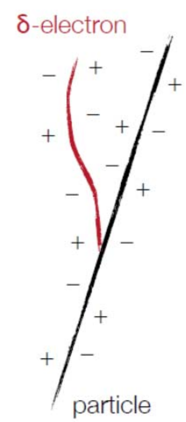

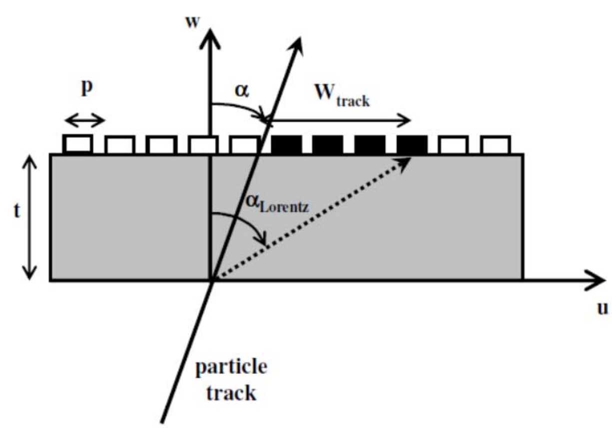

The CMS silicon inner tracker

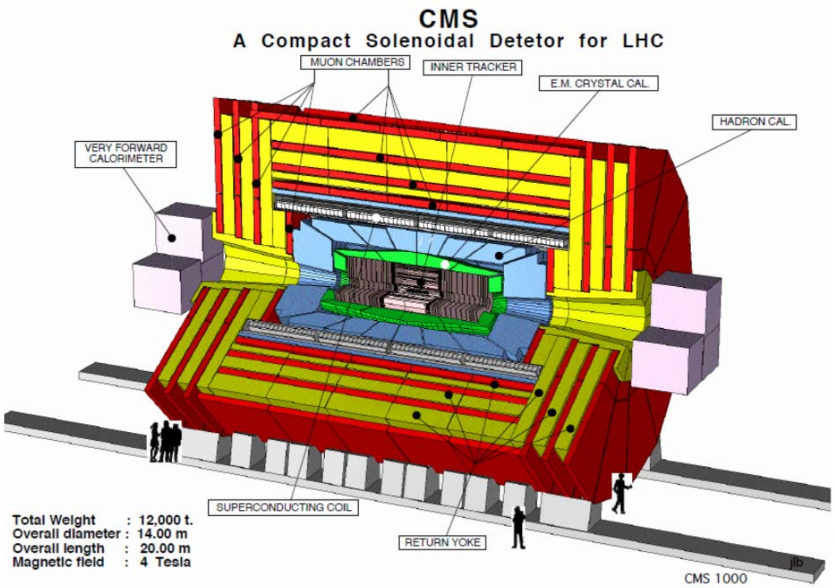

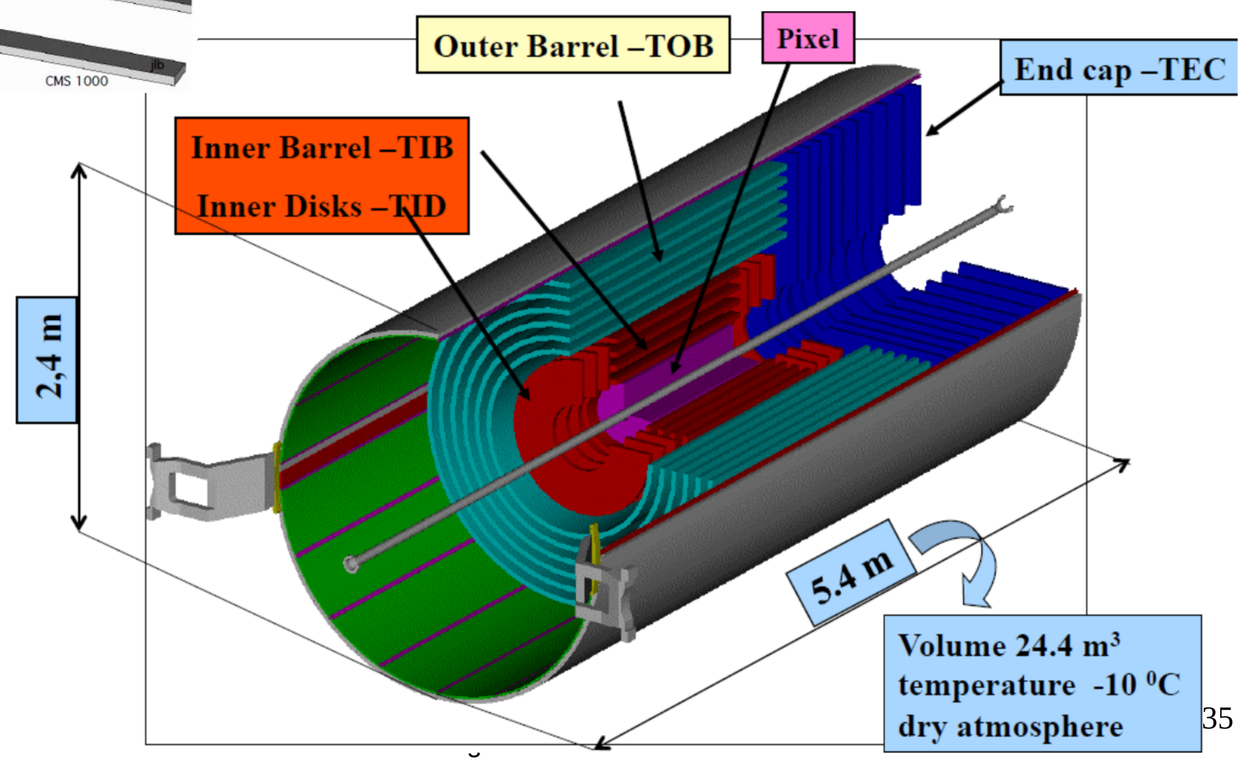

Strip detector:

~200 m^2 of silicon sensors
24,244 single silicon sensors
15,148 modules
9,600,000 strips ≡ electronics channels
75,000 read out chips (APV25)
25,000,000 Wire bonds

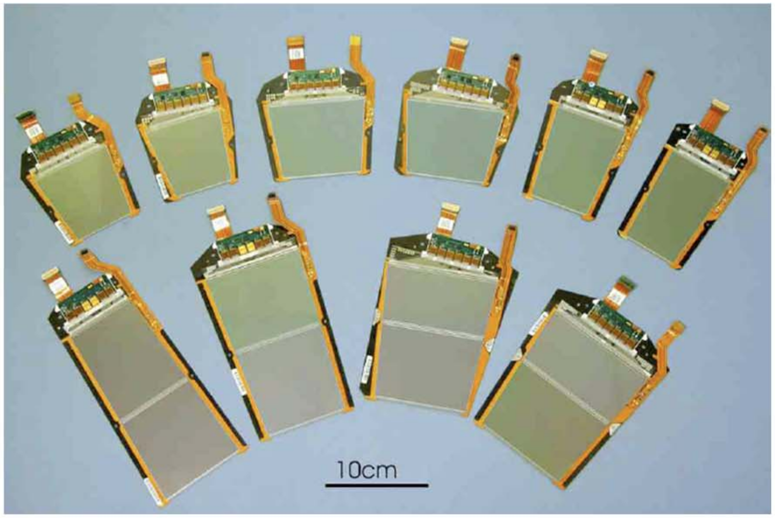

Pixel detector:

1 m^2 detector area
1440 pixel modules
66 million pixels

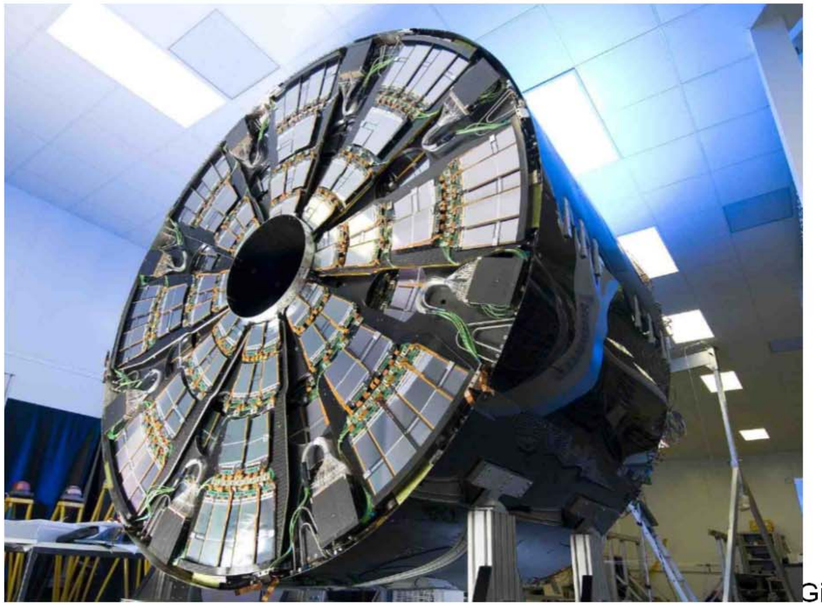

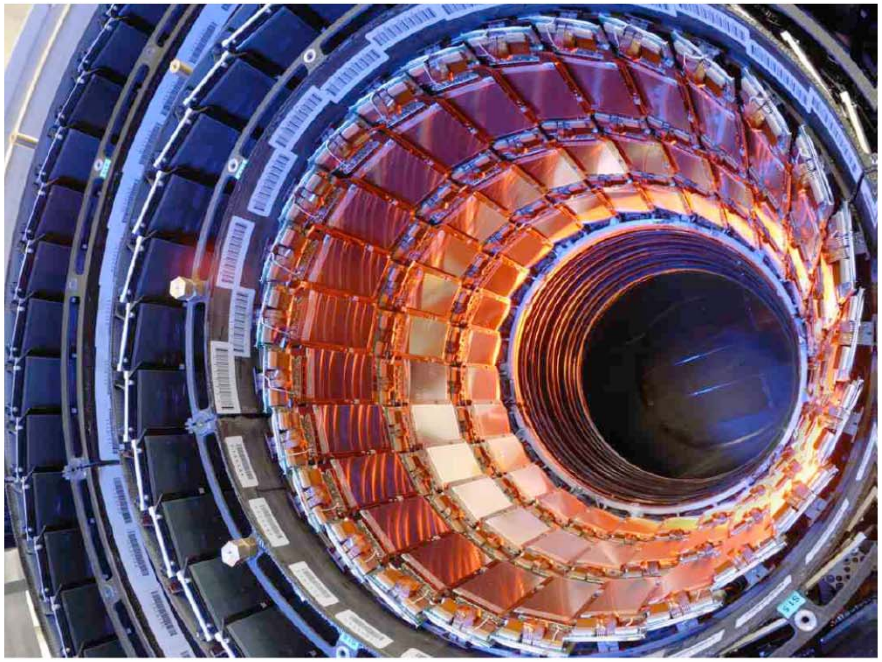

Solid state detectors: summary

- Various semiconductors
- No need for detector level charge amplification (no avalanches)
  - Small ionization energy per pair
    - E(e-h)=few eV
    - Few tens of eV in gas detectors
  - High density material
    - High energy loss
      - O(100) e-h/μm
- Time response and time resolution
  - Fast charge collection: O(10 ns)
  - Very good time resolution: O(1 ns)
- Space resolution
  - ~Pitch/√12 for digital readout
    - Pitch = 50μm-150μm
  - Much better with analog readout
    - Can make use of released charges on different strips
- Very high rate capability

TRACKING ALGORITHMS

- Experiment design
- Momentum measurement
- Track fitting

EXPERIMENT DESIGN

Detection systems

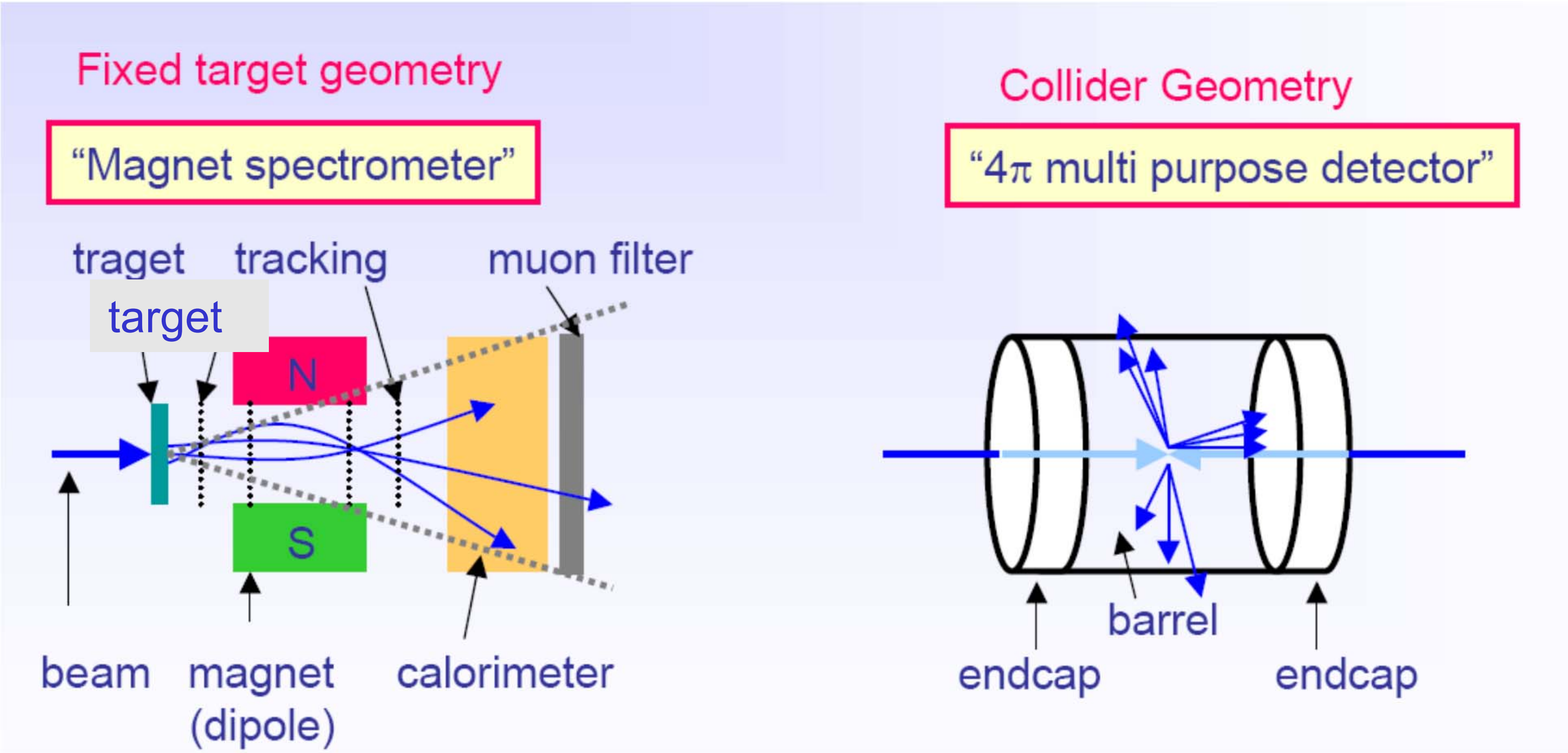

- Limited solid angle dΩ coverage
- relatively easy access (cables, maintenance)
- little energy in the center of mass
- boosted particles – very displaced secondary vertices

- "full" dΩ covergae
- very restricted access
- High energy in the center of mass

Magnetic fields in 4π experiments

UCL
Université catholique de Louvain

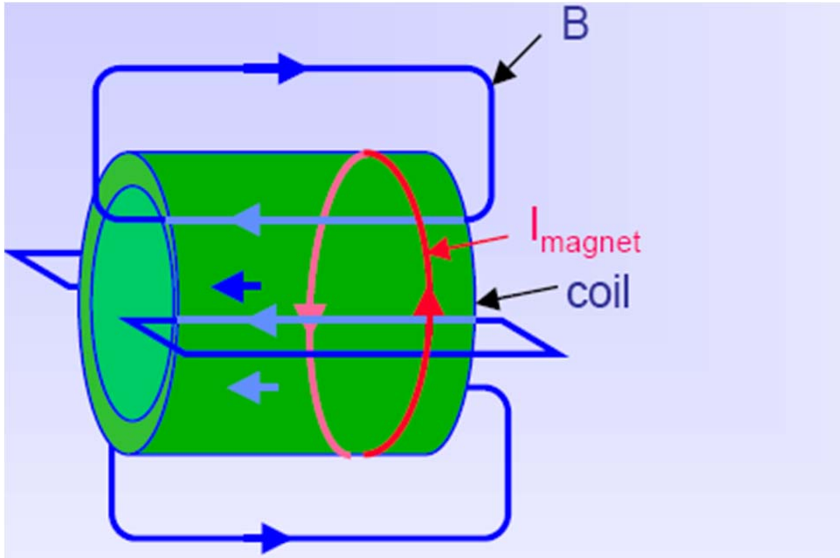

+ Large homogenous field inside coil
- weak opposite field in return yoke
- Size limited ([illegible])
- rel. high material budget

Examples:
- DELPHI: SC, 1.2T, Ø5.2m, L 7.4m
- L3: NC, 0.5T, Ø11.9m, L 11.9m
- CMS: SC, 4.0T, Ø5.9m, L 12.5m

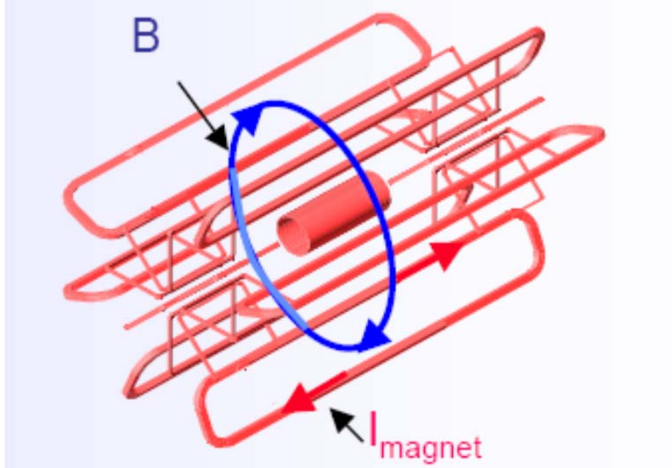

+ Field always perpendicular to $\vec{p}$
+ Rel. large fields over large volume
+ Rel. low material budget
- non-uniform field
- complex structure

Example:
- ATLAS: Barrel air toroid, SC, ~1T, Ø9.4, L 24.3m

Track bending

- Solenoidal fields
  - Bending happens in transverse plane (R-φ)
    - Will depend on transverse component of momentum only
  - Precise measurement must be in R-φ plane
  - R-z plane measurement can be less precise
- Toroidal fields
  - Bending in R-z plane
  - Cannot exploit precise knowledge of collision point at colliders

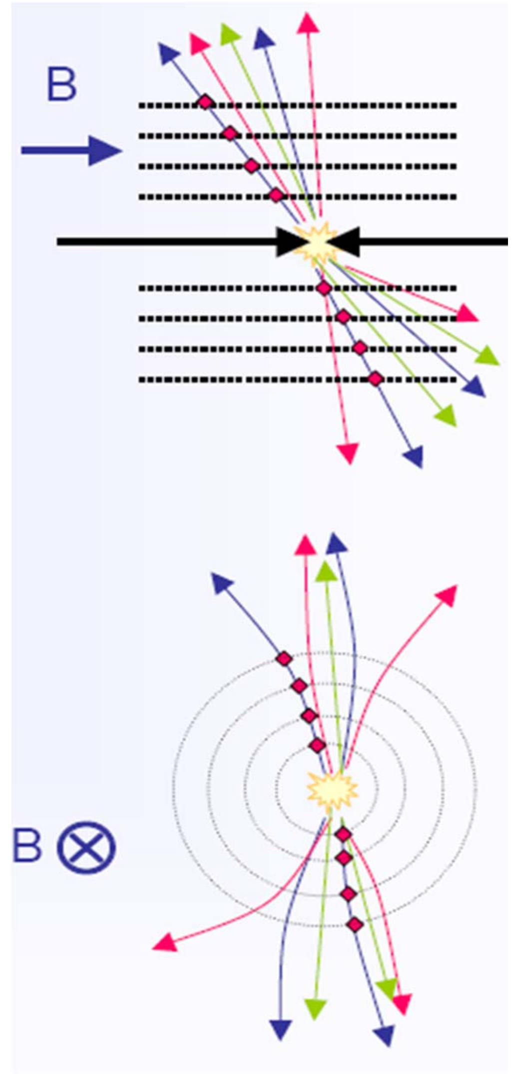

Magnets at the LHC experiments

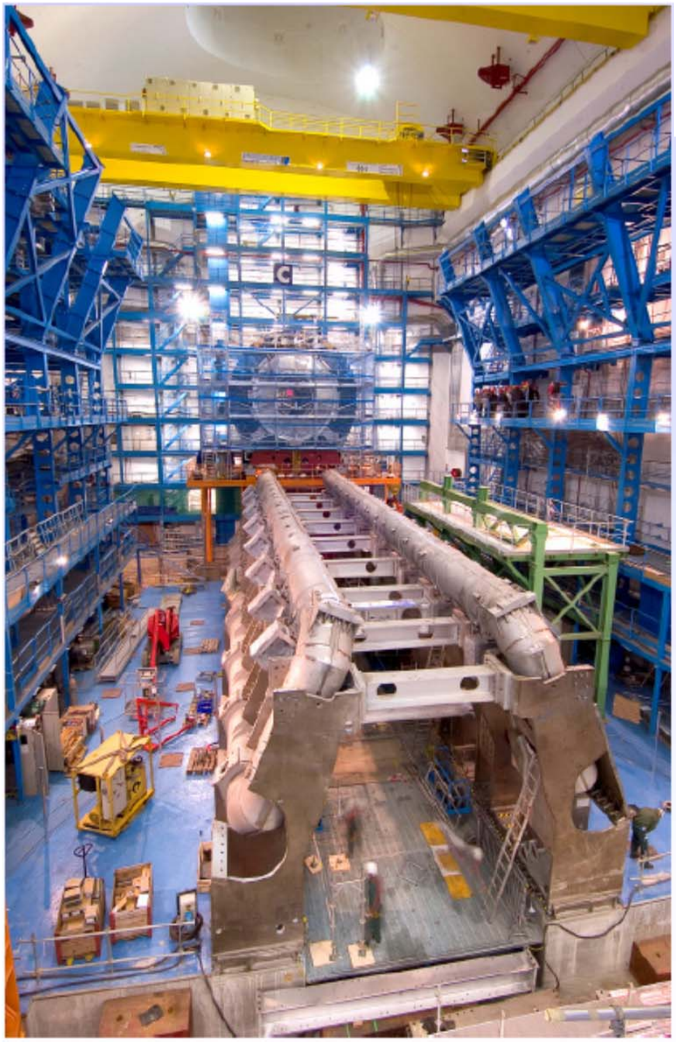

CMS Solenoid
- B=4 Tesla
- R= 2 m (1 m useful for tracking)

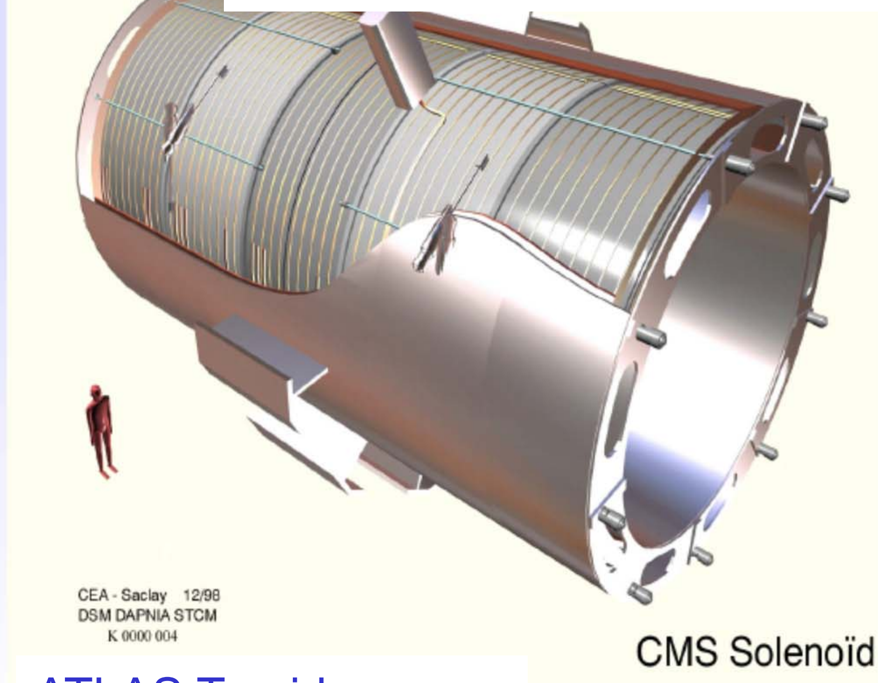

ATLAS Toroids
- B= 2 Tesla
- R= 5 m (all useful for tracking

MOMENTUM MEASUREMENT

Momentum measurement

In a solenoidal magnetic field, the transverse momentum (p_T) is measured from track curvature

- Lorentz force: $q\vec{v} \times \vec{B}$
- Trajectory is helix (projects to a circle in the transverse plane)
- p_T - classical derivation:

$$q v_T B = m \frac{{v_T}^2}{R}$$
$$p_T = qBR$$

- The same, exact result is obtained using the (correct) relativistic approach.
- In convenient units:

$$p_T[\text{GeV/c}] = 0.3B[\text{T}]\, R[\text{m}]$$

Ex: $B = 4\text{T};\ \ p_T = 100\,\frac{\text{GeV}}{\text{c}}; R = 1200\ m$

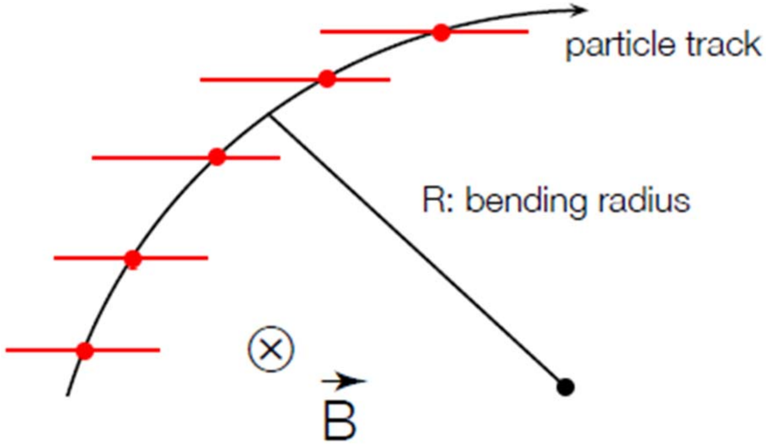

Momentum measurement uncertainty

Actual measured quantity is sagitta, *s:*

$$\left(\frac{L}{2}\right)^2 + (R-s)^2 = R^2$$

$$if\ s \ll L \quad R \approx \frac{L^2}{8s}\ ;\ p_T \approx qB\frac{L^2}{8s}$$

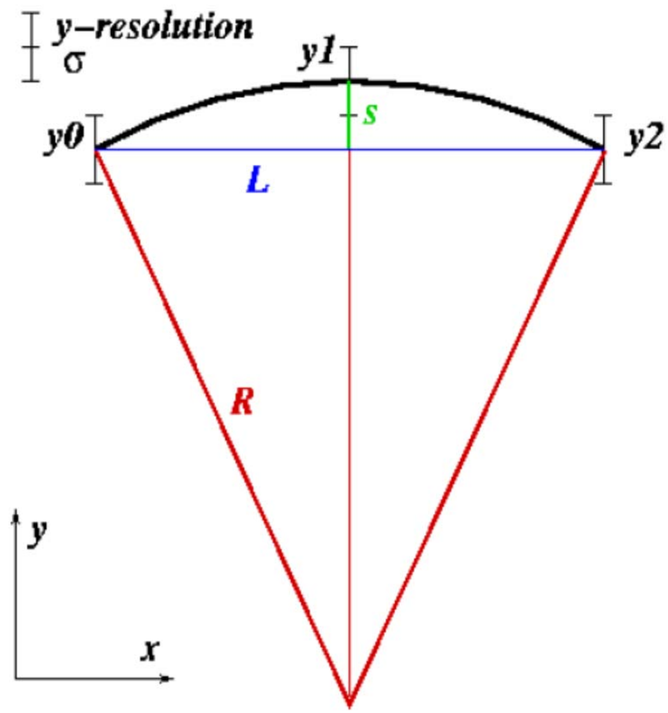

p_T relative uncertainty - error propagation :

$$\frac{\Delta p_T}{p_T} = \frac{\Delta s}{s} = \sqrt{\frac{3}{2}}\sigma_{r\varphi}\frac{8p_T}{qBL^2}$$

- prop. to detector position resolution
- prop. to p_T , $\frac{1}{B}$, $\frac{1}{L^2}$
- $\frac{1}{p_T} \propto s \rightarrow \frac{1}{p_T}$ is Gaussian distributed, not p_T

$$s = y_1 - \frac{y_0 + y_2}{2}$$

$$\Delta s = \sqrt{\frac{3}{2}}\sigma_{r\phi}$$

NB: here

$y \equiv r\phi$

If N equally spaced detectors:

$$\frac{\Delta p_T}{p_T} = \frac{a_N \sigma_{r\phi} p_T}{0.3\,BL^2};\quad a_N \approx \sqrt{\frac{720}{N+4}}$$

Uncertainty: multiple scattering

Measured change of direction:

$$|\Delta\overrightarrow{p_T}(B)| = |\overrightarrow{p_2} - \overrightarrow{p_1}| = \frac{Lp_T}{R} = 0.3BL$$

Change due to multiple scattering (MS) – assume homogeneous amount of material over distance x:

$$|\Delta\overrightarrow{p_T}(MS)| = p_T\theta_0$$

Momentum resolution due to MS:

$$\boxed{\theta_0 = \frac{13.6\ \mathrm{MeV}}{\beta cp}\, z\, \sqrt{x/X_0}\left[1 + 0.038\,\cancel{\ln(x/X_0)}\right]}$$

Using p=p_T/cosα

$$\frac{\Delta p_T}{p_T}(MS) = \frac{|\Delta\overrightarrow{p_T}(MS)|}{|\Delta\overrightarrow{p_T}(B)|} = \frac{p_T\theta_0}{0.3\ BL} \approx const \cdot \frac{\cos\alpha}{\beta BL}\sqrt{\frac{x}{X_0}}$$

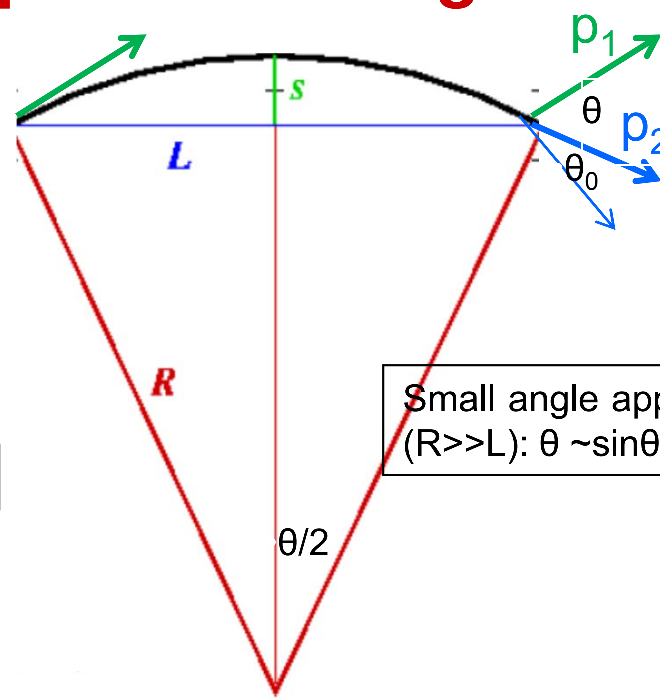

Small angle approximation (R>>L): θ ~sinθ ~ tgθ

Momentum resolution due to detector resolution:

$$\frac{\Delta p_T}{p_T}(MEAS) = const \cdot \frac{\sigma_{r\varphi}p_T}{BL^2}$$

Total momentum resolution:

$$\left(\frac{\Delta p_T}{p_T}(TOT)\right)^2 = const \cdot \left(\frac{\sigma_{r\varphi}p_T}{BL^2}\right)^2 + const \cdot \left(\frac{\cos\alpha}{\beta BL}\sqrt{\frac{x}{X_0}}\right)^2$$

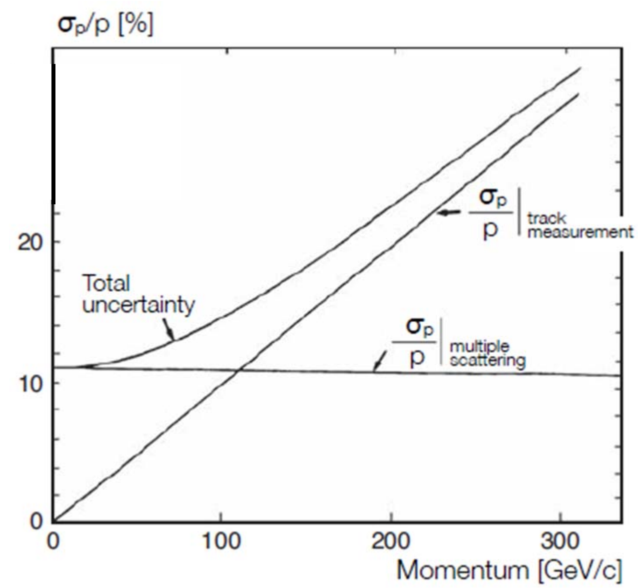

Ex(CMS tracker): $\frac{\Delta p_T}{p_T}(MS) \approx 1.5\%$ dominates up to pt~100 GeV

Uncertainty: other factors

- Energy loss by ionization is usually small and easily predictable
  - Negligible effect
  - Only in rare cases, emission of energetic δ-rays biases the measurement
- Energy loss by bremsstrahlung has large effects
  - Use calorimeter rather than tracker
    - collects brem e^- too at the same position – collinear emission
  - More sophisticated methods: evolution of Kalman Filter (will see later): Gaussian Sum Filter
    - Try to take it into account the energy loss probability.
- Contribution of measurement uncertainty in z-coordinate on full momentum measurement (not just its transverse component)
  - $p = \frac{p_T}{\cos\alpha} \rightarrow \left(\frac{\Delta p}{p}\right)_\alpha = \frac{\sin\alpha}{\cos\alpha}\Delta\alpha \sim \frac{\sigma_z}{L} = O\left(\frac{0.001\,m}{1m}\right) = 0.001$
    - Negligible with respect to contribution of uncertainty in transverse momentum

TRACK RECONSTRUCTION

- Track reconstruction classical tasks
  - Track finding
    - Determines all the subsets of detector position measurements believed to originate from the same particle: the track candidates
    - Methods classified as either “local” or “global”
  - Track fitting
    - Applies to a track candidate and aims to estimate as accurately as possible the set of parameters describing the kinematical state of the particle at some point in space, often at a reference surface close to the beam crossing point

TRACK FINDING

Track finding global method: conformal mapping

UCL Université catholique de Louvain

- Maps circles through origin to straight lines

$$(x-a)^2+(y-b)^2=r^2=a^2+b^2 \qquad u=\frac{x}{x^2+y^2},\quad v=\frac{y}{x^2+y^2}, \qquad v=\frac{1}{2b}-u\frac{a}{b}.$$

- High energy tracks almost go through origin
- Build a histogram of line azimuth-angles
- Find peaks in the histogram
- Hits in the peak are track candidates

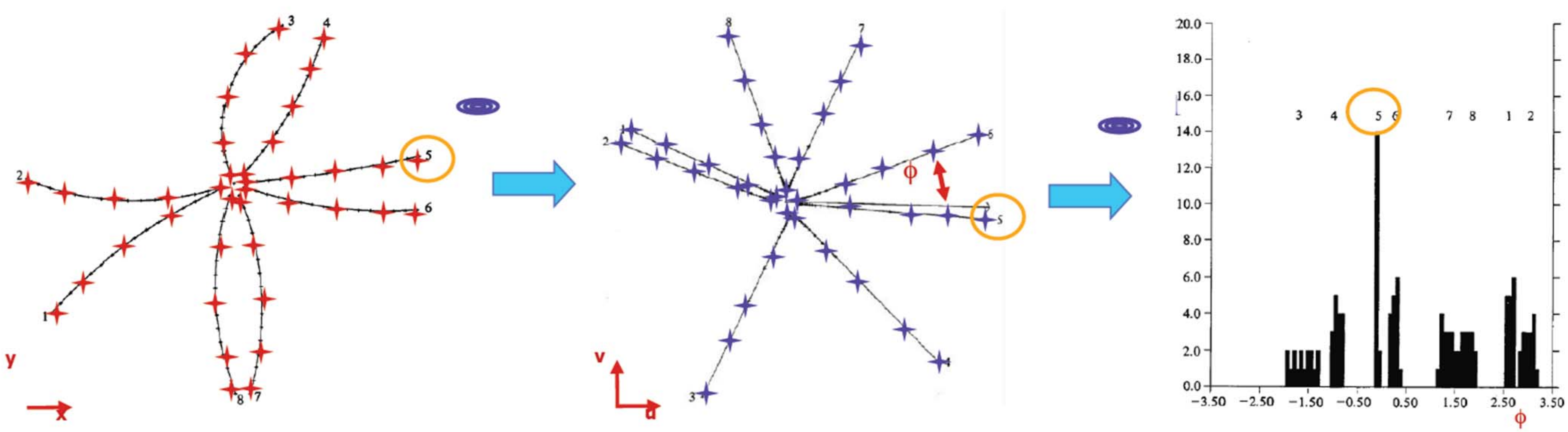

Hough and Legendre transforms

- Conformal doesn't work when tracks are not all circles through a single point. Similar, more complex, approaches can be used to for such situations:
  - ❑ Hough Transform maps straight lines to straight lines (2d point → straight line)

    $$y = cx + d \qquad d = -xc + y$$

    - Points lying on a straight line in xy plane tend to form lines in the cd plane that cross at the point providing the line parameters in xy
    - Peak search in a binned 2d parameter space yield
  - ❑ Legendre Transform maps circles to sinusoidal curves

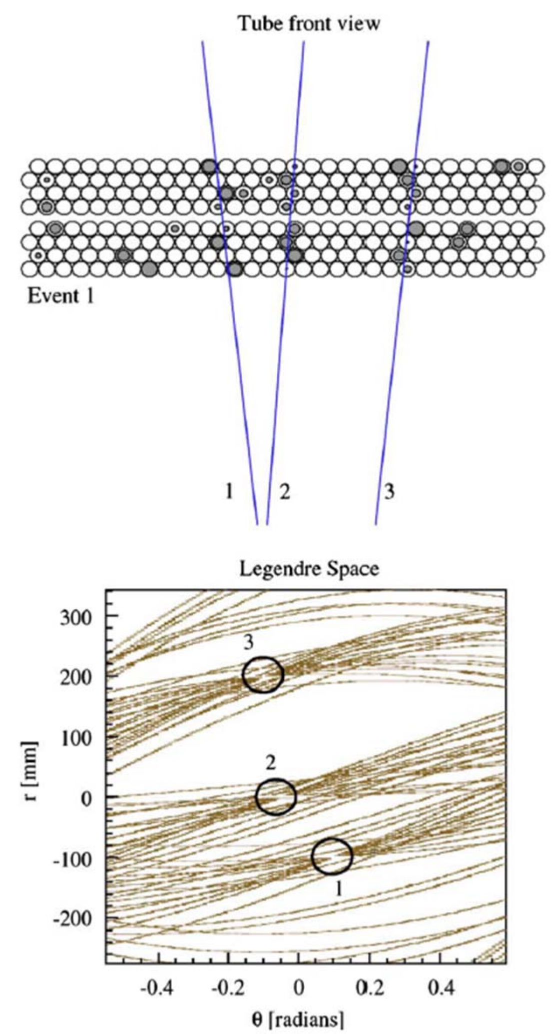

Track finding: local methods

- Track road
  - Initiated by a set of measurements that could have been originated by the same track ("seeds")
  - The expected shape of the trajectory is used to extrapolate a "road" in the tracking volume
  - Measurements within the road boundaries represent the track candidates
    - There can be more than one candidate per road
- Track following
  - Same first step as before
  - Extrapolates to next layer and picks the statistically most compatible position measurement.
  - Iterate until last layer is reached or too many detection layers with no compatible hits were checked

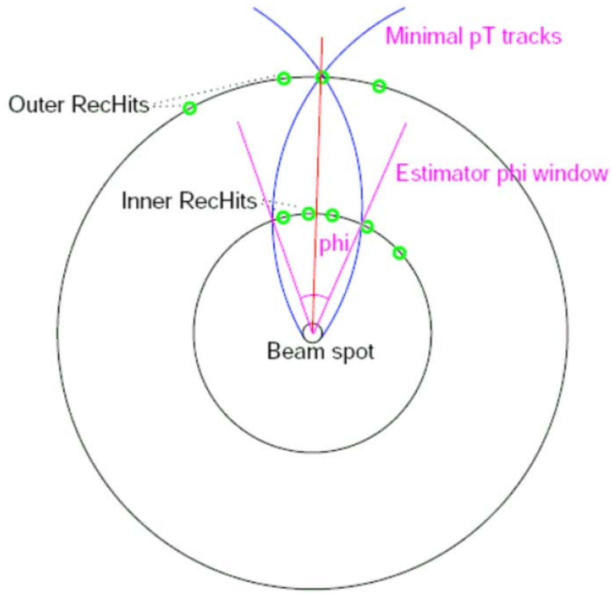

TRACK FITTING

Relevant concepts

- Track parameters
  - 5 parameters fully specify the track state at a given surfac
    - Ex: 2 coordinates on the surface + momentum (3 parameters)
    - 3rd spatial coordinate known by placement of surface
  - Why fixing a surface ? Because detector measurements are on a surface (the one identified by the detector itself – known)
- Track covariance matrix
  - 5x5 matrix describing the uncertainties in the track parameters and their correlations
    - Diagonal elements are parameter variances σ_i^2
    - Off-diagonal elements are covariance terms $\rho\sigma_i\sigma_j$, where ρ is correlation coefficient
- Track model
  - Describes how the track parameter or state vector at a given surface *k* depends on the state vector on a different surface *l*
  - Allows “propagation” of track parameters and their covariance matrix
- Detector measurements
  - Characterised by different parameters than track
    - Typically 2d points (and 2x2 cov matrix) or 2d segments (4 par)

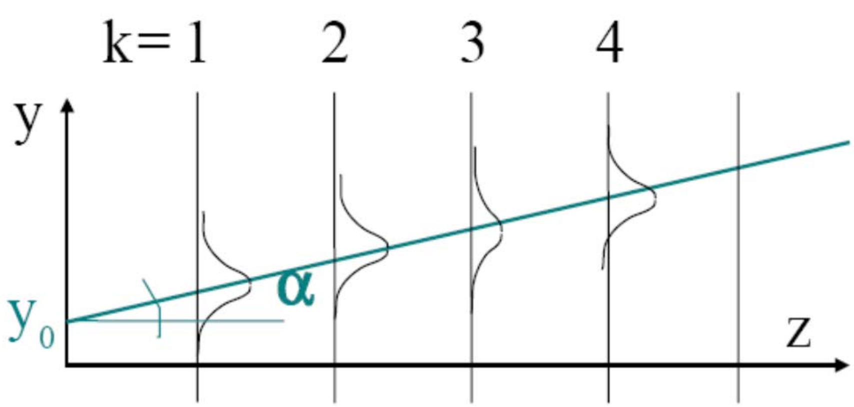

Ex: tracking in 2d with no field

Parameters $p = \binom{y}{\alpha}, m = y$

Track model

$$p_k = \begin{pmatrix} y_i + \alpha_i (z_k - z_i) \\ \alpha_i \end{pmatrix}$$

Naïve track fitting

- Examples
  - Tracking in 2d with no magnetic field
    - Fit the 1d measurements with a straight line in a 2d plane - χ^2 minimization
    - Best-fit values correspond to track parameters on first detection surface
  - Tracking in transverse plane with magnetic field
    - Fit 1d measurements with a circle (R, x_0, y_0) in the plane - χ^2 minimization
    - Best-fit values provide momentum at any point along trajectory (from R), and position at any surface (from intersection with circle)
- This approach is basically what has been assumed in the treatment of momentum measurement earlier in this course and in some simple track finding algorithms
  - Results are biased and non-optimal for having neglected material effects

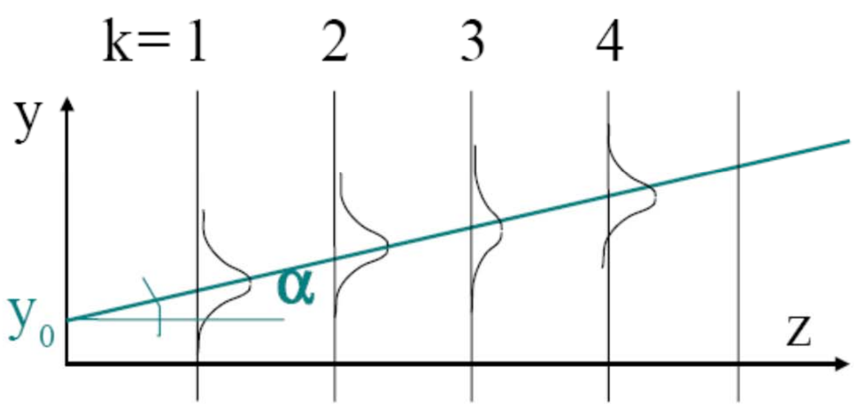

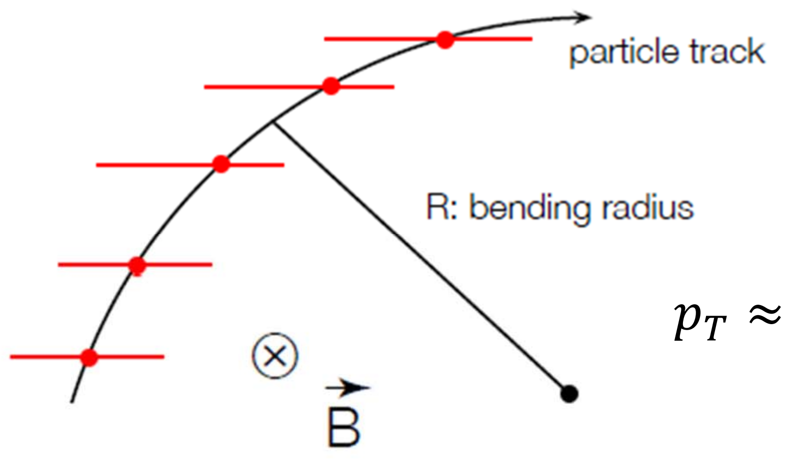

$$p_T \approx qB\,\frac{L^2}{8s}$$

Material effects and Kalman Filter

- Material effects
  - Energy loss by ionization
    - If there is B-field the particle trajectory will be bent more according to the energy lost.
    - Often modeled as a deterministic effect in the track model- neglect fluctuations
  - Multiple scattering
    - MS deflects the trajectory in a random fashion.
    - Effect results in inflated covariance matrix of after track propagation.
  - Bremsstrahlung energy loss
    - Large non-Gaussian fluctuations. Affects both track parameters and covariance matrix.
    - Cannot be treated optimally by the simplest and most common track fitting approach: **the linear global least-squares method**
- Linear global least-squares method
  - Least-squares fit to detector measurements
  - Takes into account detector effects (ionization and MS) in the track model.
  - Optimal method if true track model is linear, i.e. if propagation can be performed with a matrix operation.
- Kalman Filter algorithm
  - Iterative, equivalent, version of the global, least-squares method
  - Computationally less demanding: requires inversion of smaller matrices

Kalman Filter (KF) technique in a nutshell

1. KF starts when track hits have already been identified
   - Result of “pattern finding” step
2. KF also needs a “seed”
   - The “seed” is the track state (i.e. estimated track 3-momentum, position and associated cov matrix)at some starting surface
3. KF propagates the track state to the next surface containing a measurements
   - The track model is used to compute the extrapolated track state
4. KF “updates” the track state at the reached surface with the information from the measured hit
   - Weighted (by the uncertainties) mean of two measurements.
5. Iterate 3 to 4 until last detector surface with a measured hit is reached
6. KF “smooths” the state at previous surfaces
   - Adds information from following measurements

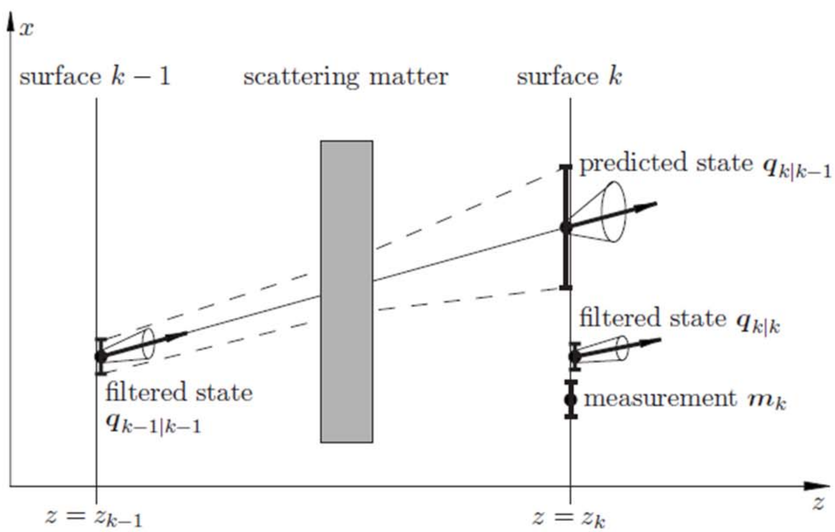

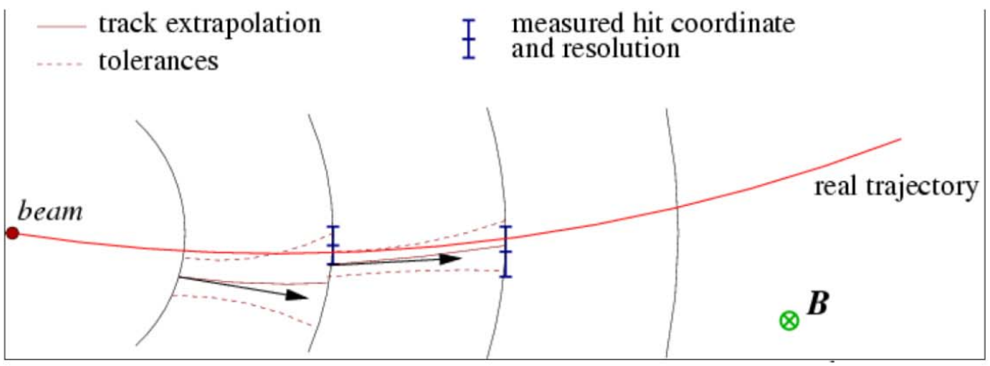

Kalman Filter technique (I)

- **"Propagation" step**
  - Propagate track state (including its uncertainty) from one surface to the next detection surface
  - $\mathbf{p_k^{k-1} = F_{k-1} p_{k-1}}$
    - $\mathbf{F_{k-1}}$ propagation matrix (5x5) from surface k-1 to next surface
      - Depends on average energy loss, magnetic field, detector layout
      - Describes the **deterministic** part of the propagation
    - $\mathbf{P_{k-1}}$ track parameters at surface k-1
    - $\mathbf{P_k^{k-1}}$ propagated track parameters from surface k-1 to surface k

    Note that this is a linear transformation
  - $\mathbf{C_k^{k-1} = F_{k-1} C_{k-1} F^T_{k-1} + Q_{k-1}}$
    - $\mathbf{C_{k-1}}$ **covariance matrix** at surface k-1
    - $\mathbf{Q_{k-1}}$ contribution to covariance matrix from random part of propagation (Multiple Scattering and energy loss)

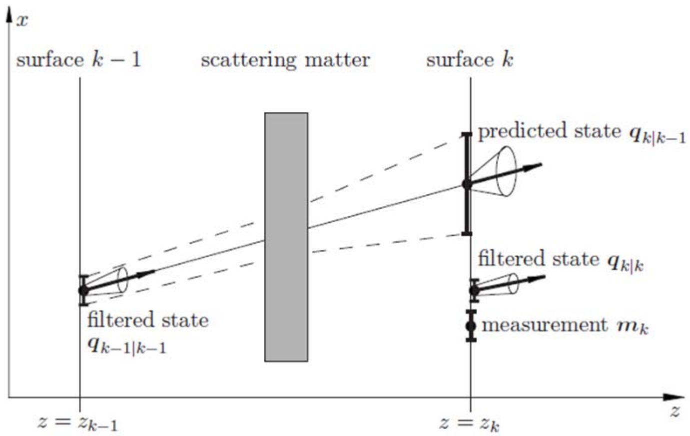

Kalman Filter technique (II)

- **"Update" step**
  - Use measurement on reached detection surface to correct extrapolated track state (weighted average of two independent measurements of the same quantity)
  - Updated state
    - $\mathbf{p_k = C_k[(C_k^{k-1})^{-1}\, p_k^{k-1} + H_k^T V_k^{-1} m_k]}$
    - $\mathbf{C_k = [(C_k^{k-1})^{-1} + H_k^T V_k^{-1} H_k]^{-1}}$
    - **H_k matrix (2x5 if 2-d detector measurements)**
      - It transforms the 5 track parameter at surface k into the 2 position-related parameters that are measured by the detector. Needed because, in general, a detector doesn't measure directly all 5 track parameters.
    - **V_k** "covariance" or error matrix of detector measurement
      - Elements of matrix V are determined on the basis of the knowledge of the used detectors (space resolution…)

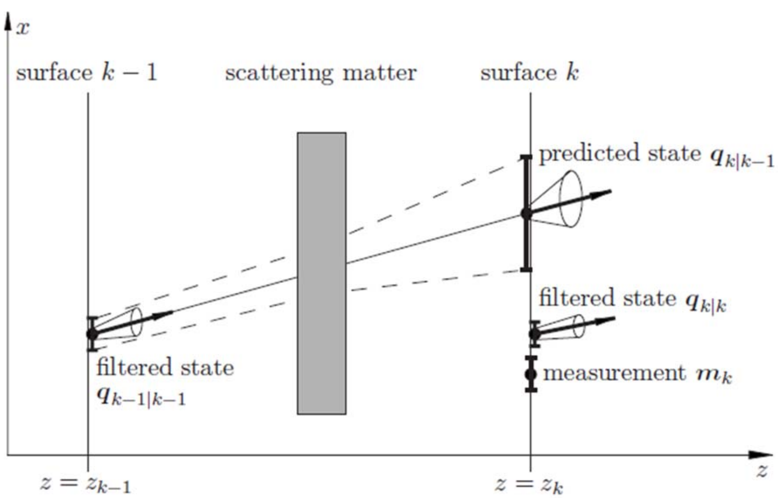

Kalman Filter (III)

- “Smoothing” step
  - Full information (measured track hits) is used only at the last surface
  - How can we use all available information to obtain the best estimate of the the track state on intermediate surfaces?
    - Once reached the last surface, perform Kalman Filter in opposite direction (“backward” as opposed to “forward”) and compute on each surface a weighted sum of the backward extrapolated state and the forward updated state
- Removal of outliers
  - From noise, other tracks… (mistakes of track finding)
  - Monitor measurement contribution to track χ^2
    - doesn’t work in presence of more than one outlier
    - Robust adaptive methods address this issue
- Resolution of ambiguities
  - Track finding can be such that two or more measurements are shared by tracks. Must resolve these cases
    - One method is Combinatorial Kalman Filter
      - Track finding and fitting steps are merged
      - Branch tracks If more than one compatible measurement is found
      - Eventually keep the best track based on quality and χ^2

VERTEX RECONSTRUCTION

Vertex reconstruction

- Vertex finding
  - Identify subsets of tracks originated from the same point in space
    - Colliding beams → primary vertices
    - Decay of unstable particles → secondary decay vertices
    - Interaction with matter → secondary interaction vertices
- Vertex fitting
  - Estimate the vertex position and the track states at some surface near the vertex
- Benefits of vertex reco
  - Use vertex constraint to improve track parameters
  - Reconstruct momentum of unstable particles decaying to charged ones
  - Measure decay lengths of unstable particles

Vertex finding

- One simple method for primary vertices
  - Take longitudinal impact parameter of all reco tracks (coordinate along beam direction of the point of closest approach to the beam line in trasverse plane) Build triplets of hits and project in the longitudinal plane (no bending) the straight line
  - Histogram them and search for maxima
- Other methods
  - Radon transform (similar to approach seen in track finding)
  - Neural network based
  - … details in reference

Vertex fitting

- Problem is very similar to track fitting
  - Track states at some refence surface are the measurements
  - The vertex position and the track momenta at the vertex are the quantities to be estimated
    - Classical method: KF vertex fitter
      - Final result does not depend on order of tracks
      - Smoother updates the track momenta with ultimate vertex position
      - Track states of participating tracks can be updated with additional vertex point. Tracks are no longer independent
- More recent efforts have gone into robust vertex fitters
  - Reduce impact of outliers.

ALIGNMENT

UCL
Université catholique de Louvain

Alignment

- The alignment problem
  - Estimate 3 shifts + 3 rotation angles per detector module
  - Vector $\mathbf{a}_k$ of alignment parameters for N modules (at the LHC $N\sim10^4$)
- Precision to achieve
  - Better than detector resolution
    - Which is much better than assembly precision plus “survey” measurements (laser based systems)
    - Need track based alignment
- Track based alignment methods
  - Residual methods
  - Least squares methods
  - Slides taken from (web link on last slide on references):

Seminar Datenverarbeitung in der Hochenergiephysik – Computing in High Energy Physics

Software Alignment for Tracking Detectors

January 17th 2005

Volker Blobel – Universität Hamburg

Toy experimental setup

Test of alignment method with a MC toy track detector model:

- 10 planes of tracking chambers, 1 m high, 10 cm distance, no magnetic field;
- accuracy $\sigma \approx 200\mu$m, with efficiency $\epsilon = 90\%$;
- plane 7 sick: accuracy $\sigma \approx 400\mu$m, with efficiency $\epsilon = 10\%$;
- 10 000 tracks with 82 000 hits available for alignment;
- Misalignment: the vertical position of the chambers are displaced by ≈ 0.1cm (normal distributed).

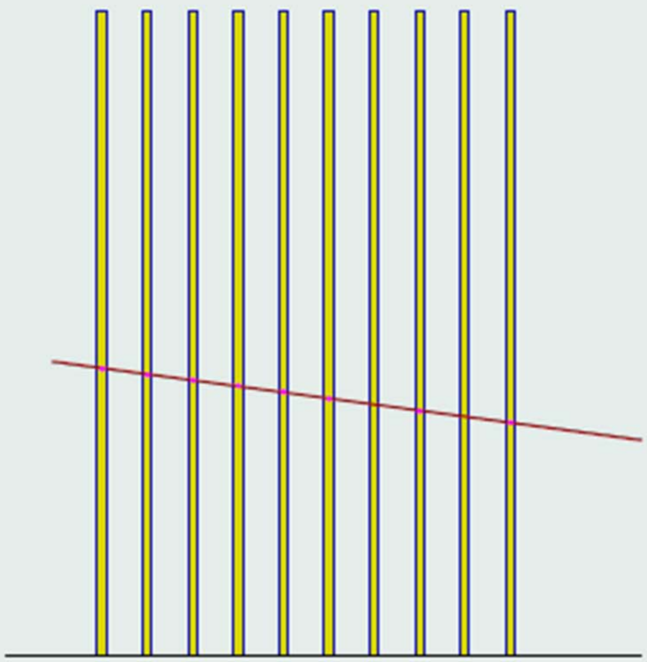

Residual methods

The first alignment attempt is based on the distribution of hit residuals:

- A straight line is fitted to the track data.
- The residuals (= measured vertical coordinate minus fitted coordinate) are histogrammed, separately for each plane.

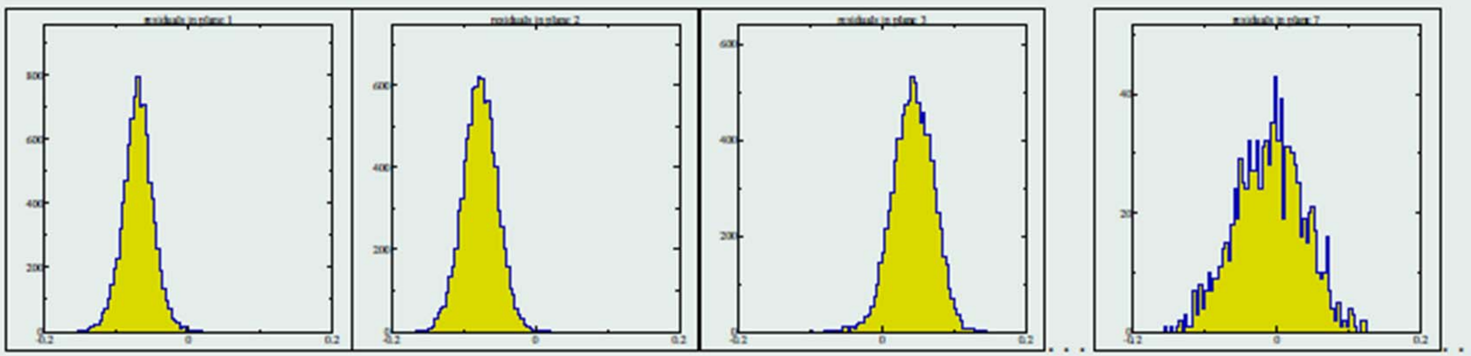

- The mean value of the residuals is taken as correction to the vertical plane position.

This is the standard method used in many experiments.

Results after 30 iterations

ID	true shift	determined	mean residual
1	0.1391	0.0727	0 ± 150
2	0.1345	0.0786	0 ± 189
3	0.0000	−0.0453	0 ± 234
4	−0.0756	−0.1102	0 ± 244
5	−0.1177	−0.1422	0 ± 205
6	0.0610	0.0475	0 ± 150
7	0.0130	0.0114	0 ± 464
8	0.0886	0.0968	0 ± 255
9	0.0000	0.0186	0 ± 149
10	−0.0467	−0.0176	0 ± 143

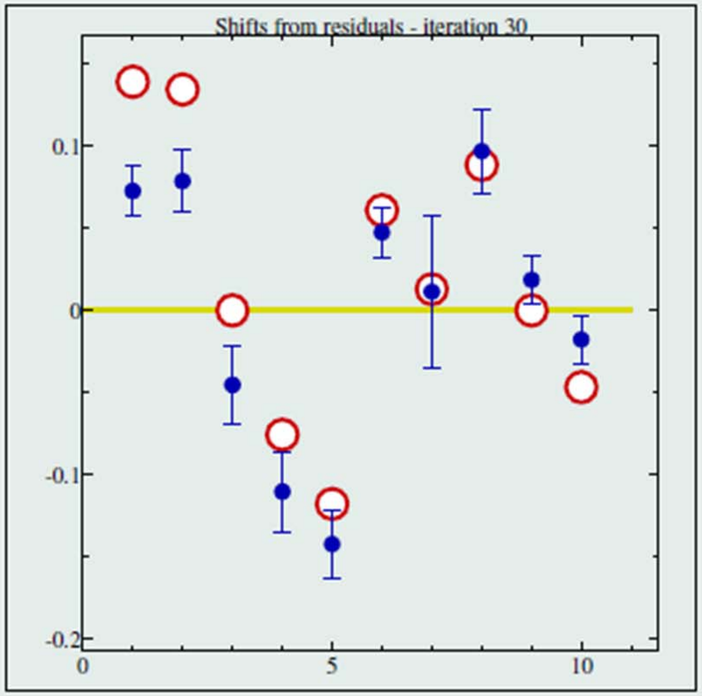

red circle = true shift (displacement)
blue disc = displacement, determined from residuum

Large changes in first iteration, small changes in second iteration, almost no progress afterwards.

Discussion

The result is not (yet) encouraging!

The reason for non-convergence is simple:

Two degrees of freedom are undefined: a simultaneous shift and a rotation of all planes!

(This simple fact is not always mentioned in reports on the method!)

Improvement for second residual attempt:

Fix the displacement (i.e. displacement = 0) of two planes, which are assumed to be carefully aligned externally (e.g. planes 3 and 9).

Other possibilities are:

- Use only fixed planes (planes 3 and 9) in the fit, and determine the residuals of other planes;
- for the determination of the displacement of a certain plane use all other planes in the fit.

These possibilities are in fact used by several collaborations!

Improved results

After 30 iterations with planes 3 and 9 fixed (displacement = 0) ...

ID	true shift	determined	mean residual
1	0.1391	0.1391	-1 ± 150
2	0.1345	0.1344	0 ± 189
3	0.0000	0	2 ± 234
4	−0.0756	−0.0758	0 ± 244
5	−0.1177	−0.1183	0 ± 205
6	0.0610	0.0607	0 ± 150
7	0.0130	0.0140	0 ± 464
8	0.0886	0.0888	0 ± 255
9	0.0000	0	0 ± 149
10	−0.0467	−0.0469	0 ± 143

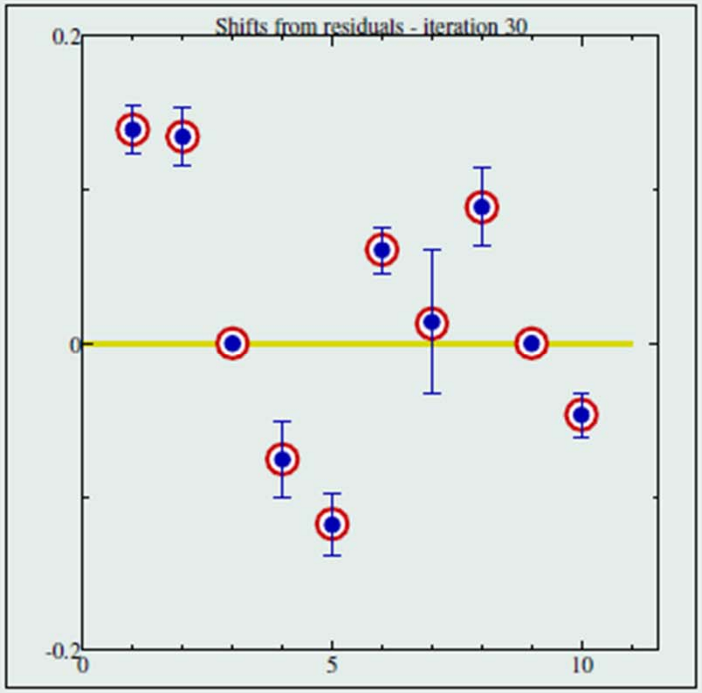

red circle = true shift (displacement)

blue disc = displacement, determined from residuum

Large changes in first iteration, then many smaller and smaller changes: convergence is **linear** and slow, because the determination of displacements is based on biased fits.

Linear least-squares method

Residual-based methods work with biased results. Can the bias be avoided by an improved fit?

Yes: include the alignment parameters in the parameters fitted in track fits – requires a simultaneous fits of many tracks, with determination of (global) alignment parameters and (local) track parameters.

model: $y_i \cong a_1^{\text{local}} + a_2^{\text{local}} \cdot x_i \quad + a_j^{\text{global}}$ $\quad a_j^{\text{global}}$ = shift for plane, where y_i is measured

1 tracks	$2 + 10 = 12$ parameters	9 equations
2 tracks	$4 + 10 = 14$ parameters	18 equations
...	...	...
10 000 tracks	20 010 parameters	82 000 equations

. . . a linear least squares problem of $m = 82\,000$ equations (measurements) and $n = 20\,010$ parameters with $n \ll m$, which requires the solution of a matrix equation with 20010-by-20010 matrix.

. . . a nice problem!

Results after one attempt

After one step (with planes 3 and 9 fixed at displacement = 0) ...

ID	true shift	determined	ρ	mean residual
1	0.1391	0.1393 ± 0.004	0.68	0 ± 150
2	0.1345	0.1346 ± 0.003	0.66	0 ± 189
3	0.0000			0 ± 234
4	−0.0756	-0.0756 ± 0.003	0.58	0 ± 244
5	−0.1177	-0.1182 ± 0.003	0.53	0 ± 205
6	0.0610	0.0608 ± 0.003	0.50	0 ± 150
7	0.0130	0.0141 ± 0.007	0.20	0 ± 464
8	0.0886	0.0888 ± 0.003	0.53	0 ± 255
9	0.0000			0 ± 149
10	−0.0467	-0.0469 ± 0.003	0.57	0 ± 143

(ρ = global correlation coefficient)

red circle = true shift (displacement)

blue disc = displacement, determined in fit

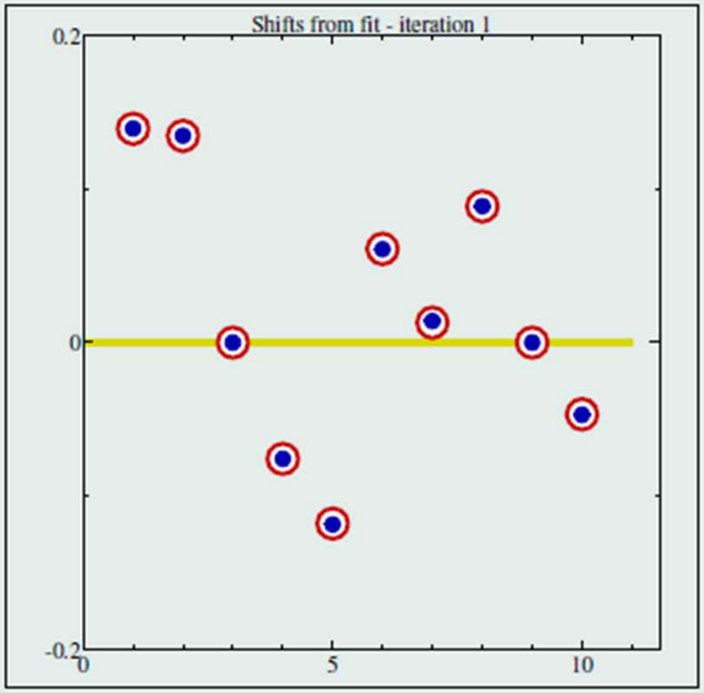

One step is sufficient: 1. step $\Delta\chi^2 = 1.277 \times 10^6$ 2. step $\Delta\chi^2 = 1.159 \times 10^{-5}$

But how can this problem be solved in less than a second?

Added value: fit detector parameters

Improvement: include, in addition, corrections to the drift velocities for each plane: $\Delta v_{\text{drift}}/v_{\text{drift}}$

$$y_i \cong a_1^{\text{local}} + a_2^{\text{local}} \cdot x_i \quad + a_j^{\text{global}} + \ell_{\text{drift},i} \cdot \left(\frac{\Delta v_{\text{drift}}}{v_{\text{drift}}}\right)_j$$

a_j^{global} = shift for plane

$\left(\frac{\Delta v_{\text{drift}}}{v_{\text{drift}}}\right)_j$ = relative v_{drift} difference

reduction of residual σ by 30 - 40 %

ID	true shift	determined	ρ	$\Delta v_{\text{drift}}/v_{\text{drift}}$	determined	ρ	mean residual
1	0.1391	0.1393 ± 0.004	0.68	0.0020	0.0019 ± 0.0002	0.016	0 ± 119
2	0.1345	0.1346 ± 0.003	0.66	-0.0153	-0.0150 ± 0.0002	0.020	0 ± 128
3	0.0000			0.0193	0.0194 ± 0.0002	0.017	0 ± 137
4	-0.0756	-0.0756 ± 0.003	0.58	0.0200	0.0197 ± 0.0002	0.013	0 ± 139
5	-0.1177	-0.1182 ± 0.003	0.53	-0.0138	-0.0136 ± 0.0002	0.013	0 ± 141
6	0.0610	0.0608 ± 0.003	0.50	0.0003	0.0004 ± 0.0002	0.019	0 ± 139
7	0.0130	0.0141 ± 0.007	0.20	-0.0306	-0.0303 ± 0.0006	0.038	0 ± 348
8	0.0886	0.0888 ± 0.003	0.53	0.0237	0.0238 ± 0.0002	0.018	0 ± 134
9	0.0000			-0.0044	-0.0044 ± 0.0002	0.008	0 ± 127
10	-0.0467	-0.0469 ± 0.003	0.57	0.0021	0.0019 ± 0.0002	0.013	0 ± 117

. . . this would be rather difficult with a pure residual-based method.

References

- Tracking detectors
  - textbook: Glenn F. Knoll, “Radiation Detection and Measurement”, John Wiley & Sons, 16 August 2010 - 860 pages
- Momentum measurement
  - R.L.Gluckstern, Nucl. Inst r. and Meth. 24 (1963) 381
- Tracking, vertexing and alignment
  - Review paper: A. Strandlie and R. Frühwirth, “Track and vertex reconstruction: From classical to adaptive methods”, Rev. Mod. Phys. 82, 1419–1458 (2010). References therein
  - Alignment talk by V.Blobel: http://www.desy.de/~blobel/altalk.pdf